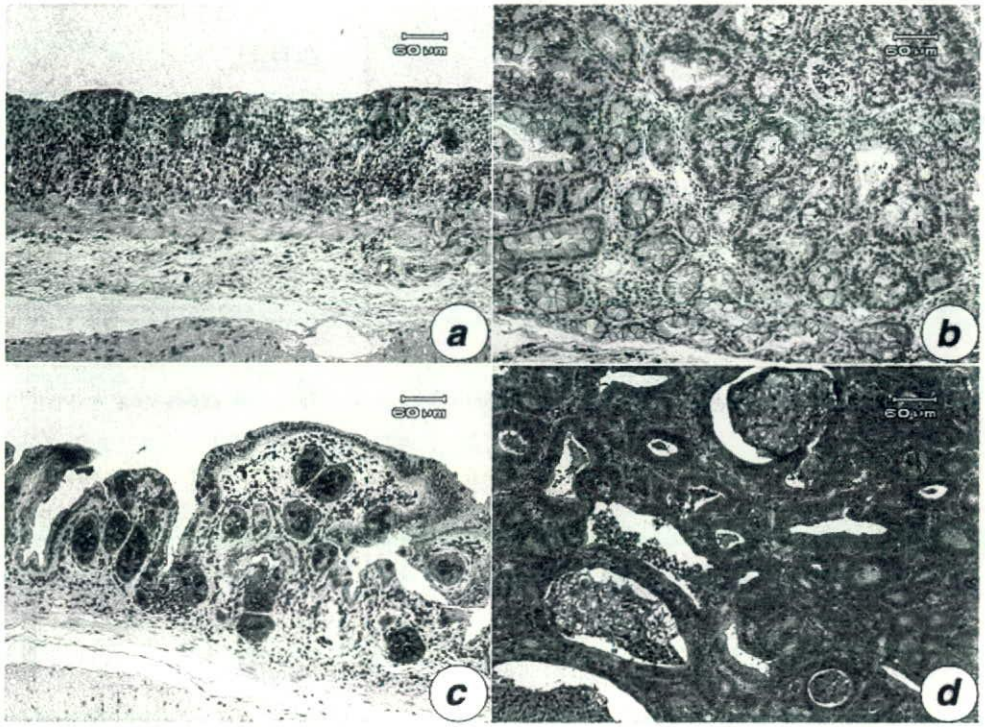

FIGURE 4 – Immunohistochemistry of NF-κB (*a, b*) and HO-1 (*c, d*). Strong NF-kB expression is observed in (*a*) mononuclear inflammatory cells in the colonic mucosa and (*b*) colonic ADC cells. HO-1 expression is relatively weak in (*c*) mononuclear inflammatory cells in the colonic mucosa and strong in (*d*) some of ADC cells. Bars in the photos indicate magnification (μm).

TABLE III – EFFECTS OF DIETARY ZERUMBONE ON THE DEVELOPMENT OF LUNG PROLIFERATIVE LESIONS INDUCED BY NNK (EXP. 2)

Group no.	Treatment	No. of mice examined	Incidence (%)			Multiplicity (no. of prolierative lesions/lung)		
			HP	AD	Total	HP	AD	Total
1	NNK[1]	12	100[2]	100[2]	100	2.75 ± 0.97[3,4]	8.25 ± 2.83[4]	11.00 ± 2.92[4]
2	NNK+100 ppm ZER	10	70	100	100	1.50 ± 1.18[5]	6.40 ± 2.63	7.90 ± 2.64
3	NNK+250 ppm ZER	10	40[6]	90	90	0.50 ± 0.71[7]	4.70 ± 3.33[5]	5.20 ± 3.74[7]
4	NNK+500 ppm ZER	10	90	80	90	0.90 ± 0.32[7]	2.60 ± 2.17[7]	3.50 ± 2.32[7]
5	500 ppm ZER	5	40	20	40	0.40 ± 0.55	0.20 ± 0.45	0.60 ± 0.89
6	Untreated	5	40	40	60	0.40 ± 0.55	0.60 ± 0.89	1.00 ± 1.22

[1]NNK, 4-(methylnitrosamino)-1-(3-pyridyl)-1-butanone; HP, hyperplasia; AD, adenoma; and ZER, zerumbone.–[2]Significantly different from the untreated group (group 6) by Fisher's exact probability test ($p = 0.0147$).–[3]Mean ± SD.–[4]Significantly different from the untreated group (group 6) by Tukey-Kramer multiple comparison posttest ($p < 0.001$).–[5]Significantly different from the NNK group (group 1) by Tukey-Kramer multiple comparison posttest ($p < 0.05$).–[6]Significantly different from the NNK group (group 1) by Fisher's exact probability test ($p = 0.0028$).–[7]Significantly different from the NNK group (group 1) by Tukey-Kramer multiple comparison posttest ($p < 0.001$).

Exp. 2: Effect of ZER on NNK-induced lung carcinogenesis

General observation. Any clinical signs of toxicity of dietary ZER were not noted during the experiment. At sacrifice, the mean weight of lungs of the NNK-treated mice (group 1, 0.45 ± 0.05 g, $p < 0.05$) was significantly greater than that of the untreated mice (group 6, 0.35 ± 0.02 g). The mean weight of lungs of the mice in groups 2 (0.39 ± 0.05 g, $p < 0.05$), 3 (0.35 ± 0.05 g, $p < 0.05$), and 4 (0.36 ± 0.03 g, $p < 0.05$) were significantly lower as compared with that of group 1. Other measures (body, liver, kidney and spleen weights) did not significantly differ among the groups.

Effects of dietary ZER on the development of lung proliferative lesions. Table III summarizes the data on the incidence and multiplicity of lung proliferative lesions (HP and AD) induced by NNK and/or ZER. All mice belonging to group 1 developed alveolar cell HP and AD (Fig. 2*b*) with 100% incidences ($p = 0.0147$ for each) with high multiplicities of HP (2.75 ± 0.97, $p < 0.001$) and AD (8.25 ± 2.83, $p < 0.001$), as compared with an untreated group (group 6). Dietary ZER slightly affected the incidences of lung HP and AD, but significantly lowered the multiplicity of HP (100 ppm ZER: 1.50 ± 1.18, $p < 0.05$; 250 ppm ZER: 0.50 ± 0.71, $p < 0.001$; and 500 ppm ZER: 0.90 ± 0.32, $p < 0.001$) as compared group 1. Likewise, the supplementation of ZER at 250 (4.70 ± 3.33, $p < 0.05$) and 500 ppm (2.60 ± 2.17, $p < 0.001$) to the diet significantly reduced the multiplicity of AD when compared to group 1. The inhibition by 100 ppm ZER feeding was insignificant. Suppression effects of ZER at 3 dose levels demonstrated an inverse relationship of inhibition in the multiplicity of lung AD (Pearson $r = -0.9855$, $p < 0.00145$).

Effects of ZER on proliferation and apoptosis of lung ADs. As shown in Figure 5, ZER feeding at 250 ppm ($p < 0.01$) and 500 pmm ($p < 0.001$) significantly decreased the PCNA-labeling index of adenoma cells (Fig. 5*a*) and significantly increased TUNEL-positive apoptotic nuclei ($p < 0.01$ at 100 and 250 ppm, and $p < 0.001$ at 500 ppm) of lung adenoma cells (Fig. 5*b*).

Immunohistochemical scores of NFκB and HO-1 in lung ADs. Positive immunohistochemical reactions of NFκB (Fig. 6*a*) and HO-1 (Fig. 6*c*) were observed in lung adenomas that developed in NNK-treated mice. The positive reactions were reduced in

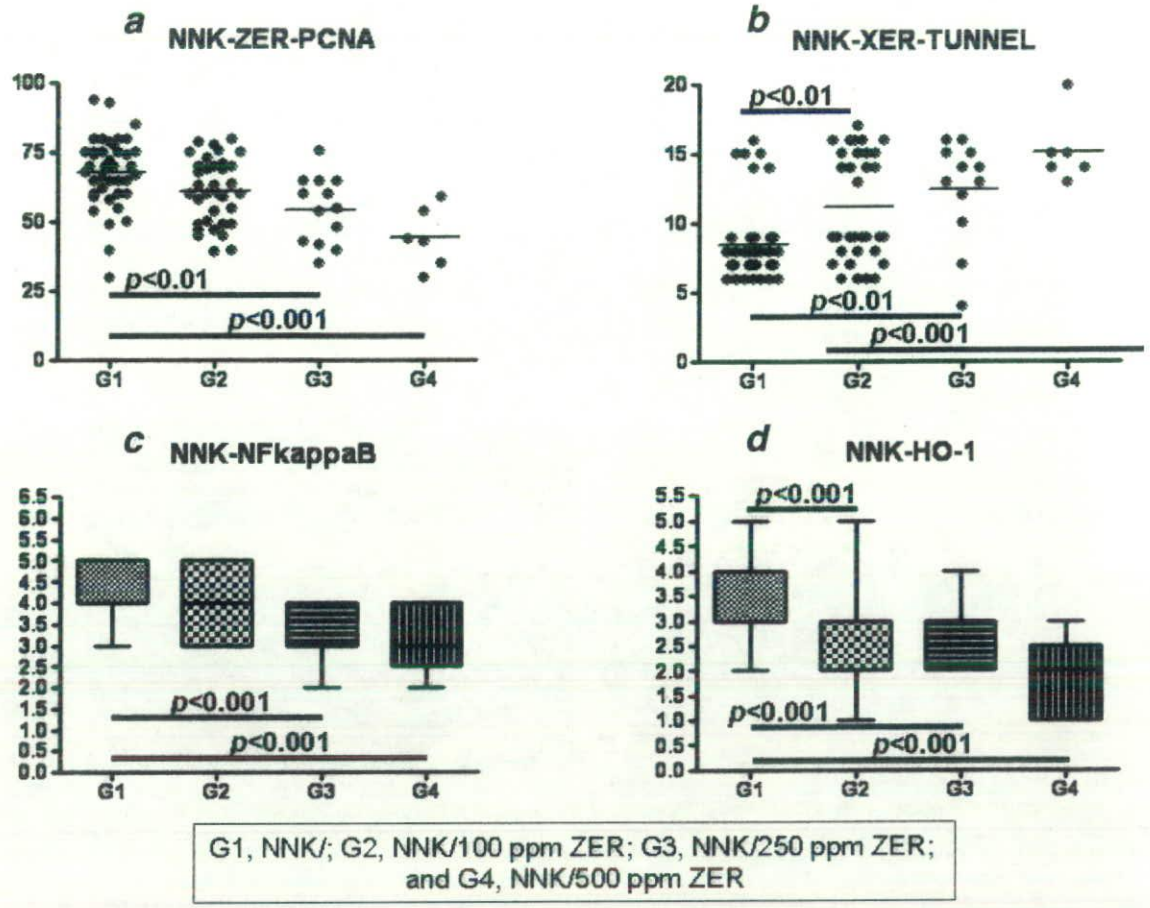

FIGURE 5 – Immunohistochemical scores of (*a*) PCNA-labeling index, (*b*) apoptotic index, (*c*) NF-κB and (*d*) HO-1, which were determined in lung adenoma developed in mice of groups 1 through 4.

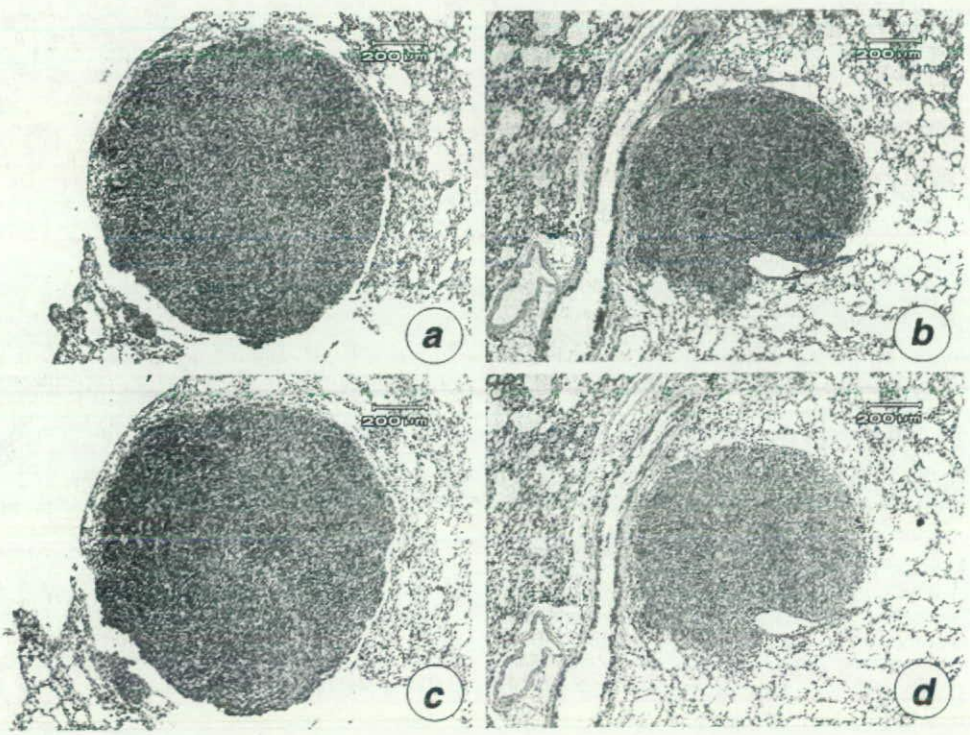

FIGURE 6 – Representative immunohistochemical reactions of NF-κB (*a*, *b*) and HO-1 (*c*, *d*) of lung adenomas. While strong reactivities of (*a*) NF-κB and (*c*) HO-1 are observed in the lung adenoma from group 1 (NNK alone), those of (*c*) NF-κB and (*c*) HO-1 from group 4 (NNK + 500 ppm ZER) are weak.

the lung AD (Figs. 6*b* and 6*d*) of mice that received NNK and ZER. As illustrated in Figure 5, feeding with ZER dose-dependently reduced the immunohistochemical scores and the inhibition of the NF-kB score (Fig. 5*c*) by ZER at 250 ($p < 0.001$) and 500 ppm ($p < 0.001$) and that of the HO-1 score (Fig. 5*d*) by ZER at 100 ($p < 0.001$), 250 ($p < 0.001$) and 500 ppm ($p < 0.001$) were statistically significant.

Discussion

The findings described here clearly indicated the chemopreventive effects of ZER derived from wild ginger in the mouse colon and lung carcinogenesis models. The protective ability of ZER is considered to be mediated by its anti-proliferative, apoptosis-inducing, anti-inflammatory and suppression of NF-kB and HO-1 expression. Together with our previous findings,[4,28] ZER is one of the possible chemopreventive agents against carcinogenesis in different tissues, including colon, lung and skin.[28] As large amount of ZER is readily available from the rhizomes of *Z. zerumbet*, further investigations for clarifying for detailed mechanisms of inhibition can be conducted in multiple organs of preclinical and clinical chemopreventive studies.

We assessed in this study chemopreventive ability of ZER at 3 dose levels (100, 250 and 500 ppm in diet) using 2 different mouse carcinogenesis models. All doses of ZER suppressed colonic inflammation and reduced the multiplicity of colonic ADC formation induced by AOM/DSS in a dose-dependent manner. In the NNK-induced lung tumorigenesis, ZER at all doses reduced the multiplicity of proliferative lesions, HP and ADs. The suppressing effects of ZER on the multiplicity of lung ADs showed clear dose-dependency. Importantly, we did not observe any toxicity of ZER in 2 different experiments.

As expected from our previous study[4] showing the inhibitory effects of ZER on the development of AOM-induced ACF, which is putative precursor lesion for colonic ADCs,[29,30] dietary ZER inhibited the occurrence of colonic ADC induced by the AOM/DSS treatment. Although the model system of colitis-related colon carcinogenesis[16] used in this study to induce colonic preneoplastic and neoplastic lesions was different from that for sporadic CRC,[4,29,30] protective effects of ZER on colon tumorigenesis are more likely in the inflamed colon, where the risk for ADC development is quite high.[31] Previous *in vitro* and *in vivo* investigations revealed strong anti-inflammatory properties of ZER.[1–3,5,28,32,33] Moreover, ZER can induce detoxifying enzymes.[34] ZER, thus, might be a cancer chemopreventive agent for the high-risk groups for CRC, such as ulcerative colitis and patients who receive polypectomy or surgical resection of CRC.

NF-κB is the key transcriptional factor for synthesis of proinflammatory mediators, including iNOS, COX-2 and TNF-α. NF-κB also plays central roles in carcinogenesis and inflammation,[21] and thus it is one of the molecular targets of cancer chemoprevention and therapy.[24,35] In fact, NF-κB activation is reported to be involved in colon[36] and lung carcinogenesis[37] and certain NF-κB inhibitors are able to suppress cancer development in these tissues.[38,39] In this study, dietary administration of ZER reduced the immunohistochemical expression of NFκB in colonic and lung tumors. Also, we observed that ZER causes suppression of cell proliferation, and induction of apoptosis. ZER is reported to suppress proinflammatory protein production and oxidative/nitrosative stress, and to induce apoptosis in human colon cancer cell lines *via* suppressing the expression of COX-2 and iNOS.[2] ZER induces nuclear localization of nuclear factor-erythroid 2-related factor (Nrf)-2 that binds to antioxidant response element (ARE) of the phase II enzyme genes, suggesting that ZER is a potential activator of the Nrf-2/ARE-dependent phase II enzyme genes, including manganese superoxide dismutase (MnSOD), γ-glutamylcysteine glutathione peroxidase (GPx) 1[28] and HO-1.[34] In the current study, dietary feeding with ZER inhibited the immunohistochemical expression of HO-1 in the tumors developed in the colon and lung. Both *MnSOD* and *GPx1* are regulated, at least in part, by Nrf-2 transcription factor.[40] Therefore, ZER may induce these genes' expression *via* possibly Nrf-2 activation An anti-oxidative enzyme, HO-1, is protective against oxidative stress in the damaged tissues without neoplastic alterations.[41] However, overexpression of HO-1 is observed in preneoplastic[42] and neoplastic tissues[43–45] to growth and to survive against cancer therapy.[44] In this context, the effects of ZER on the expression of NF–κB and HO-1 in tumors developed in the colon and lung are of interest. We observed that dietary ZER effectively inhibits immunohistochemical expression of colonic ADCs and lung AD, suggesting that ZER has cancer chemopreventive as well as cancer chemotherapeutic potentials.

In the current experiments, we noted that ZER treatment induces apoptosis in the neoplasms of colon and lung. ZER is previously reported to induce apoptosis in a variety of colon cancer cell lines (LS174, LS180, COLO205 and COLO320DM) with different degree.[2] The α,β-unsaturated carbonyl group of ZER is suspected to be responsible for the effects.[2] A recent report by Sakinah *et al.*[46] showing that ZER treatment results in decreased expression of the anti-apoptotic protein Bcl-2 and increased the expression of the pro-apoptotic protein Bax in human hepatocellular cancer cells, HepG2, confirmed apoptosis-inducing effects of ZER in malignant epithelial cells.

In conclusion, our findings indicate that a sesquiterpenoid, zerumbone, being a major constituent of the subtropical ginger plant *Zingiber zerumbet* Smith is one of the good candidates with multiple targets for cancer chemopreventive agent in colon and lung carcinogenesis related with inflammation.

Acknowledgements

This work was supported in part by a Grant-in-Aid (to T.T. and Y.Y.) for Scientific Research from the Ministry of Education, Culture, Sports, Science and Technology of Japan; and grants (to T.T. and Y.Y.) for the Project Research from the High-Technology Center of Kanazawa Medical University.

References

1. Murakami A, Takahashi M, Jiwajinda S, Koshimizu K, Ohigashi H. Identification of zerumbone in Zingiber zerumbet Smith as a potent inhibitor of 12-O-tetradecanoylphorbol-13-acetate-induced Epstein-Barr virus activation. Biosci Biotechnol Biochem 1999;63:1811–2.
2. Murakami A, Takahashi D, Kinoshita T, Koshimizu K, Kim HW, Yoshihiro A, Nakamura Y, Jiwajinda S, Terao J, Ohigashi H. Zerumbone, a Southeast Asian ginger sesquiterpene, markedly suppresses free radical generation, proinflammatory protein production, and cancer cell proliferation accompanied by apoptosis: the alpha,beta-unsaturated carbonyl group is a prerequisite. Carcinogenesis 2002;23:795–802.
3. Murakami A, Hayashi R, Tanaka T, Kwon KH, Ohigashi H, Safitri R. Suppression of dextran sodium sulfate-induced colitis in mice by zerumbone, a subtropical ginger sesquiterpene, and nimesulide: separately and in combination. Biochem Pharmacol 2003;66:1253–61.
4. Tanaka T, Shimizu M, Kohno H, Yoshitani S, Tsukio Y, Murakami A, Safitri R, Takahashi D, Yamamoto K, Koshimizu K, Ohigashi H, Mori H. Chemoprevention of azoxymethane-induced rat aberrant crypt foci by dietary zerumbone isolated from Zingiber zerumbet. Life Sci 2001;69:1935–45.
5. Murakami A, Matsumoto K, Koshimizu K, Ohigashi H. Effects of selected food factors with chemopreventive properties on combined lipopolysaccharide- and interferon-gamma-induced IkappaB degradation in RAW264.7 macrophages. Cancer Lett 2003;195:17–25.
6. Takada Y, Murakami A, Aggarwal BB. Zerumbone abolishes NF-kappaB and IkappaBalpha kinase activation leading to suppression of antiapoptotic and metastatic gene expression, upregulation of apoptosis, and downregulation of invasion. Oncogene 2005;24:6957–69.

7. Balkwill F, Mantovani A. Inflammation and cancer: back to Virchow? Lancet 2001;357:539–45.
8. Azad N, Rojanasakul Y, Vallyathan V. Inflammation and lung cancer: roles of reactive oxygen/nitrogen species. J Toxicol Environ Health B Crit Rev 2008;11:1–15.
9. Engels EA. Inflammation in the development of lung cancer: epidemiological evidence. Expert Rev Anticancer Ther 2008;8:605–15.
10. Lala PK, Chakraborty C. Role of nitric oxide in carcinogenesis and tumour progression. Lancet Oncol 2001;2:149–56.
11. Wogan GN, Hecht SS, Felton JS, Conney AH, Loeb LA. Environmental and chemical carcinogenesis. Semin Cancer Biol 2004;14:473–86.
12. Xie J, Itzkowitz SH. Cancer in inflammatory bowel disease. World J Gastroenterol 2008;14:378–89.
13. Itzkowitz SH, Yio X. Inflammation and cancer IV. Colorectal cancer in inflammatory bowel disease: the role of inflammation. Am J Physiol Gastrointest Liver Physiol 2004;287:G7–17.
14. Hecht SS, Hoffmann D. Tobacco-specific nitrosamines, an important group of carcinogens in tobacco and tobacco smoke. Carcinogenesis 1988;9:875–84.
15. Kim M, Miyamoto S, Sugie S, Yasui Y, Ishigamori-Suzuki R, Murakami A, Nakagama H, Tanaka T. A tobacco-specific carcinogen, NNK, enhances AOM/DSS-induced colon carcinogenesis in male A/J mice. In Vivo, in press.
16. Tanaka T, Kohno H, Suzuki R, Yamada Y, Sugie S, Mori H. A novel inflammation-related mouse colon carcinogenesis model induced by azoxymethane and dextran sodium sulfate. Cancer Sci 2003;94:965–73.
17. Hecht SS, Hochalter JB, Villalta PW, Murphy SE. 2'-Hydroxylation of nicotine by cytochrome P450 2A6 and human liver microsomes: formation of a lung carcinogen precursor. Proc Natl Acad Sci U S A 2000;97:12493–7.
18. Hecht SS, Morse MA, Amin S, Stoner GD, Jordan KG, Choi CI, Chung FL. Rapid single-dose model for lung tumor induction in A/J mice by 4-(methylnitrosamino)-1-(3-pyridyl)-1-butanone and the effect of diet. Carcinogenesis 1989;10:1901–4.
19. Yao R, Rioux N, Castonguay A, You M. Inhibition of COX-2 and induction of apoptosis: two determinants of nonsteroidal anti-inflammatory drugs' chemopreventive efficacies in mouse lung tumorigenesis. Exp Lung Res 2000;26:731–42.
20. Prawan A, Kundu JK, Surh YJ. Molecular basis of heme oxygenase-1 induction: implications for chemoprevention and chemoprotection. Antioxid Redox Signal 2005;7:1688–703.
21. Maeda S, Omata M. Inflammation and cancer: role of nuclear factor-kappaB activation. Cancer Sci 2008;99:836–42.
22. Naugler WE, Karin M. NF-kappaB and cancer-identifying targets and mechanisms. Curr Opin Genet Dev 2008;18:19–26.
23. Miyamoto S, Epifano F, Curini M, Genovese S, Kim M, Ishigamori-Suzuki R, Yasui Y, Sugie S, Tanaka T. A novel prodrug of 4'-geranyloxy-ferulic acid suppresses colitis-related colon carcinogenesis in mice. Nutr Cancer, in press.
24. Surh YJ. NF-kappa B and Nrf2 as potential chemopreventive targets of some anti-inflammatory and antioxidative phytonutrients with anti-inflammatory and antioxidative activities. Asia Pac J Clin Nutr 2008;17 (Suppl. 1):269–72.
25. Cooper HS, Murthy SN, Shah RS, Sedergran DJ. Clinicopathologic study of dextran sulfate sodium experimental murine colitis. Lab Invest 1993;69:238–49.
26. Ward JM. Morphogenesis of chemically induced neoplasms of the colon and small intestine in rats. Lab Invest 1974;30:505–13.
27. Nikitin AY, Alcaraz A, Anver MR, Bronson RT, Cardiff RD, Dixon D, Fraire AE, Gabrielson EW, Gunning WT, Haines DC, Kaufman MH, Linnoila RI, et al. Classification of proliferative pulmonary lesions of the mouse: recommendations of the mouse models of human cancers consortium. Cancer Res 2004;64:2307–16.
28. Murakami A, Tanaka T, Lee JY, Surh YJ, Kim HW, Kawabata K, Nakamura Y, Jiwajinda S, Ohigashi H. Zerumbone, a sesquiterpene in subtropical ginger, suppresses skin tumor initiation and promotion stages in ICR mice. Int J Cancer 2004;110:481–90.
29. Tanaka T, Miyamoto S, Suzuki R, Yasui Y. Chemoprevention of colon carcinogenesis in dietary non-nutritive compounds. Curr Topics Neutraceut Res 2006;4:127–52.
30. Tanaka T, Sugie S. Inhibition of colon carcinogenesis by dietary non-nutritive compounds. J. Toxicol Pathol 2007;20:215–35.
31. Tanaka T, Kohno H, Murakami M, Shimada R, Kagami S. Colitis-related rat colon carcinogenesis induced by 1-hydroxy-anthraquinone and methylazoxymethanol acetate (Review). Oncol Rep 2000;7:501–8.
32. Murakami A, Miyamoto M, Ohigashi H. Zerumbone, an anti-inflammatory phytochemical, induces expression of proinflammatory cytokine genes in human colon adenocarcinoma cell lines. Biofactors 2004;21:95–101.
33. Murakami A, Shigemori T, Ohigashi H. Zingiberaceous and citrus constituents, 1'-acetoxychavicol acetate, zerumbone, auraptene, and nobiletin, suppress lipopolysaccharide-induced cyclooxygenase-2 expression in RAW264.7 murine macrophages through different modes of action. J Nutr 2005;135:2987S–92S.
34. Nakamura Y, Yoshida C, Murakami A, Ohigashi H, Osawa T, Uchida K. Zerumbone, a tropical ginger sesquiterpene, activates phase II drug metabolizing enzymes. FEBS Lett 2004;572:245–50.
35. Gopalakrishnan A, Kong AN. Anticarcinogenesis by dietary phytochemicals: cytoprotection by Nrf2 in normal cells and cytotoxicity by modulation of transcription factors NF-kappa B and AP-1 in abnormal cancer cells. Food Chem Toxicol 2008;46:1257–70.
36. Clemo NK, Collard TJ, Southern SL, Edwards KD, Moorghen M, Packham G, Hague A, Paraskeva C, Williams AC. BAG-1 is up-regulated in colorectal tumour progression and promotes colorectal tumour cell survival through increased NF-kappaB activity. Carcinogenesis 2008;29:849–57.
37. Stathopoulos GT, Sherrill TP, Cheng DS, Scoggins RM, Han W, Polosukhin VV, Connelly L, Yull FE, Fingleton B, Blackwell TS. Epithelial NF-kappaB activation promotes urethane-induced lung carcinogenesis. Proc Natl Acad Sci USA 2007;104:18514–9.
38. Rajakangas J, Misikangas M, Päivärinta E, Mutanen M. Chemoprevention by white currant is mediated by the reduction of nuclear beta-catenin and NF-kappaB levels in Min mice adenomas. Eur J Nutr 2008;47:115–22.
39. Anto RJ, Mukhopadhyay A, Shishodia S, Gairola CG, Aggarwal BB. Cigarette smoke condensate activates nuclear transcription factor-kappaB through phosphorylation and degradation of IkappaB(alpha): correlation with induction of cyclooxygenase-2. Carcinogenesis 2002;23:1511–8.
40. Lee JM, Calkins MJ, Chan K, Kan YW, Johnson JA. Identification of the NF-E2-related factor-2-dependent genes conferring protection against oxidative stress in primary cortical astrocytes using oligonucleotide microarray analysis. J Biol Chem 2003;278:12029–38.
41. Abraham NG, Tsenovoy PL, McClung J, Drummond GS. Heme oxygenase: a target gene for anti-diabetic and obesity. Curr Pharm Des 2008;14:412–21.
42. Lee J, Lee SK, Lee BU, Lee HJ, Cho NP, Yoon JH, Choi HR, Lee SK, Kim EC. Upregulation of heme oxygenase-1 in oral epithelial dysplasias. Int J Oral Maxillofac Surg 2008;37:287–92.
43. Kim HR, Kim S, Kim EJ, Park JH, Yang SH, Jeong ET, Park C, Youn MJ, So HS, Park R. Suppression of Nrf2-driven heme oxygenase-1 enhances the chemosensitivity of lung cancer A549 cells toward cisplatin. Lung Cancer 2008;60:47–56.
44. Loboda A, Was H, Jozkowicz A, Dulak J. Janus face of Nrf2-HO-1 axis in cancer—friend in chemoprevention, foe in anticancer therapy. Lung Cancer 2008;60:1–3.
45. Maines MD, Abrahamsson PA. Expression of heme oxygenase-1 (HSP32) in human prostate: normal, hyperplastic, and tumor tissue distribution. Urology 1996;47:717–33.
46. Sakinah SA, Handayani ST, Hawariah LP. Zerumbone induced apoptosis in liver cancer cells via modulation of Bax/Bcl-2 ratio. Cancer Cell Int 2007;7:4.

Angiotensin II Induces Oxidative Stress in Prostate Cancer

Hiroji Uemura,[1] Hitoshi Ishiguro,[1] Yukari Ishiguro,[2] Kouji Hoshino,[1] Satoru Takahashi,[3] and Yoshinobu Kubota[1]

[1]Department of Urology and [2]Department of Biology and Function in the Head and Neck, Yokohama City University Graduate School of Medicine, Yokohama, Japan and [3]Department of Experimental Pathology and Tumor Biology, Nagoya City University Graduate School of Medical Sciences, Nagoya, Japan

Abstract

Angiotensin II has been shown to be a cytokine especially acting as a growth factor. A local renin-angiotensin system has been identified in the prostate gland, and the physiologic function of angiotensin II seems to be similar in prostate cancer, as we previously reported. In the present study, we explored the biological role of angiotensin II in oxidative stress of prostate cancer cells. Activated Akt was determined, and the expression of oxidative stress-related proteins (p47phox, manganese superoxide dismutase 2, glutathione peroxidase) was examined by Western blotting in LNCaP cells, which were stimulated with angiotensin II and/or an angiotensin II receptor type 1 blocker, candesartan. To examine DNA damage induced by angiotensin II, 8-hydroxy-2′-deoxyguanosine was determined, and Western blots were analyzed to detect checkpoint proteins including p53, Chk2, and cdc2. Immunocytochemical studies of inducible nitric oxide synthase and superoxide anion radical (O_2^-) were done in LNCaP cells stimulated with angiotensin II. The phosphorylation of Akt was induced by angiotensin II treatment and inhibited by candesartan, as well as by LY294002, an inhibitor of phosphoinositide 3-kinase. Oxidative stress-related proteins were up-regulated by angiotensin II and inhibited by pretreatment with candesartan or catalase. The level of 8-hydroxy-2′-deoxyguanosine was increased by angiotensin II and conversely decreased by candesartan. Immunocytochemical studies showed that angiotensin II enhanced an inflammatory marker, inducible nitric oxide synthase, and the production of O_2^- radical. The hypothesis that angiotensin II has the potential to induce oxidative stress, which may be implicated in carcinogenesis of the prostate gland through long-term exposure to chronic inflammation is proposed. (Mol Cancer Res 2008;6(2):250–8)

Introduction

Prostate cancer is a major public health problem in men and the second leading cause of cancer death in the United States and Western developed countries (1). Recently, the prevalence of prostate cancer has also been increasing in Japan. Although the etiology has not been clarified, a possible cause is considered to be the westernization of the diet and life-style in Japan. At present, prostate cancer is thought to have a multifactorial etiology, with both environmental and genetic factors. We previously reported some genetic changes in prostate cancer cells and tissue detected using differential display method or GeneChip analysis. For example, the *liplin-α2* and *nmt55* genes have been identified using differential display method. The *liplin-α2* gene was down-regulated by dihydrotestosterone in prostate cancer cells, and the *nmt55* gene was up-regulated in prostate cancer tissue (2, 3). Also, we found that *neuroserpin* (*protease inhibitor 12*) expression was higher in prostate cancer than in normal prostate tissue by GeneChip analysis (4). Although numerous investigators have examined and identified genes related to prostate cancer, the mechanisms of prostate cancer development and progression remain obscure.

Because Virchow discovered leukocytes in neoplastic tissues and made the first connection between inflammation and cancer, the association of chronic inflammation with the development of cancer has been well recognized (5, 6). Under chronic inflammation, the release of reactive oxygen species (ROS) and reactive nitrogen species influences DNA damage in proliferating epithelium, leading to permanent genomic alterations, such as point mutations, deletions, or rearrangements (7). Oxidative or nitrosative stress occurs when excessive ROS and/or reactive nitrogen species are produced, overcoming cellular antioxidant defenses. Recently, a large number of investigations have consolidated the evidence that oxidative stress is implicated in carcinogenesis of the prostate gland. There have been accumulated reports indicating a reduction of antioxidant defense (8-10), elevated levels of ROS-related and reactive nitrogen species–related enzymes (11, 12), and

Received 6/20/07; revised 9/27/07; accepted 10/4/07.
Grant support: 2007 Strategic Research Project K19028 of Yokohama City University, grant-in-aid for Scientific Research from Ministry of Education, Culture, Science, and Technology, and COE research grant from Japan Society for the Promotion of Science.
The costs of publication of this article were defrayed in part by the payment of page charges. This article must therefore be hereby marked *advertisement* in accordance with 18 U.S.C. Section 1734 solely to indicate this fact.
Requests for reprints: Hiroji Uemura, Department of Urology, Yokohama City University School of Medicine, 3-9 Fukuura, Kanazawa-ku, Yokohama 236-0004, Japan. Phone: 81-45-787-2679; Fax: 81-45-786-5775. E-mail: hu0428@med.yokohama-cu.ac.jp

doi:10.1158/1541-7786.MCR-07-0289

increased levels of hydrogen peroxide (11) in prostatic intraepithelial neoplasia (PIN) and cancer. Nevertheless, the cause of oxidative stress linked to prostatic carcinogenesis has not been clarified.

Angiotensin II, which is a major effector peptide of the renin-angiotensin system (RAS), is well known to be an important factor in hypertension. The classic RAS has been identified in the kidney, heart, and vessel walls and characterized in terms of blood pressure and electrolyte/fluid homeostasis. On the other hand, involvement of a local RAS, with autocrine/paracrine roles rather than endocrine roles, has recently been documented in relation to growth/differentiation in specific organs. Interestingly, these phenomena also seem to occur in several cancer cells in which a local RAS is involved in the progression of cancer (13, 14). Recently, we have reported that angiotensin II affects the signal pathways in prostate cancer cells. Angiotensin II activates the signal transduction of mitogen-activated protein kinase and signal transducers and activators of transcription 3 and angiogenesis in prostate cancer cells (15). Also, angiotensin II facilitates the secretion of some growth factors and cytokines from prostate stromal cells, resulting in cell proliferation of prostate cancer (16). Of interest, many investigators have clarified that angiotensin II induces oxidative stress in vascular cells. Angiotensin II stimulates the production of ROS in endothelial cells by up-regulating the subunits of $NAD^+/NADP^+$ (NADPH) oxidases (17, 18).

Apart from the attention RAS has attracted in relation to its roles in the circulation, another function of local RAS related to cell proliferation and angiogenesis has recently been focused on, especially in carcinogenesis. To confirm the postulate that angiotensin II would induce ROS in prostate cancer cells, we examined the expression of oxidative stress-related proteins and DNA damage induced by angiotensin II and/or an angiotensin II receptor type 1 blocker (ARB). Our results support the hypothesis that angiotensin II generated in the prostate gland may be a cause of oxidative stress linked to prostatic carcinogenesis.

Results

Time Courses of Akt Phosphorylation

In the male reproductive system, the angiotensin II concentration in semen is higher than that in blood (19), which is important for enhancement of sperm motility and perforation of the oocyte. Earlier investigation of semen extender showed that 10 μmol/L angiotensin II increased retention of spermatozoa (20), and another report indicated that 100 nmol/L angiotensin II stimulated the acrosome reaction in spermatozoa (19). Therefore, 10 μmol/L angiotensin II may not be a high level in a physiologic condition. As we previously reported, 10 μmol/L angiotensin II stimulated the cell growth of prostate cancer cells in LNCaP and DU145 cells (14). Akt has been implicated in the regulation of a variety of signal transduction pathways, including those involved in cell proliferation (9, 21-23). To confirm the activation of Akt in LNCaP cells treated with angiotensin II, we did a time-course Western blot analysis. As shown in Fig. 1, phosphorylated Akt was time-dependently enhanced by 10 μmol/L angiotensin II treatment. Activation of Akt was shown from 1 h after the start of angiotensin II stimulation and gradually increased until 24 h. This phenomenon is different from the patterns of phosphorylations of mitogen-activated protein kinase and signal transducers and activators of transcription 3 shown in our previous report (14).

We then did Western blot to confirm the inhibition of Akt phosphorylation induced by angiotensin II. Figure 2A shows that Akt phosphorylation was induced in a dose-dependent manner by angiotensin II treatment at 1 and 10 μmol/L for 3 h. The Akt phosphorylation induced by 10 μmol/L angiotensin II was inhibited by pretreatment with 1 and 10 μmol/L candesartan, an ARB, for 30 min (Fig. 2B). Also, the Akt phosphorylation induced by 10 μmol/L angiotensin II was completely inhibited by pretreatment with 40 μmol/L LY294002, an inhibitor of phosphoinositide 3-kinase for 30 min (Fig. 2C). Also, pretreatment with 1,000 units/mL catalase, an antioxidant enzyme, for 30 min inhibited the Akt phosphorylation induced by 10 μmol/L angiotensin II for 3 h in LNCaP cells (Fig. 2D).

Expression of AT1 Receptor in LNCaP Cells

To confirm expression of the angiotensin II receptor type-1 receptor AT1 receptor, LNCaP cells were treated with 10 μmol/L angiotensin II for 24 h. As shown in Fig. 3, expression of the AT1 receptor was enhanced by angiotensin II treatment. Unlike Akt phosphorylation shown in Fig. 2, expression of the AT1 receptor was not inhibited by pretreatment with 10 μmol/L candesartan (CV11974) or 1,000 units/mL catalase for 30 min. Therefore, this result indicates that candesartan and catalase do not influence the expression of the AT1 receptor in LNCaP cells.

Expression of Oxidative Stress-Related Proteins Induced by Angiotensin II and ARB Treatment

We then did Western blot to examine whether oxidative stress-related proteins were affected when prostate cancer cells (LNCaP) were stimulated by angiotensin II treatment. Besides the major generation of ROS by mitochondrial respiration, superoxide is also generated by a family of enzymes known as NADPH oxidases, and p47phox is a crucial cytosolic regulatory subunit of NADPH oxidases. The expression of p47phox protein was enhanced by 10 μmol/L angiotensin II treatment for 24 h, as shown in Fig. 4 (*top*). As anticipated, this augmentation of p47phox expression was inhibited by pretreatment with 10 μmol/L candesartan or 1,000 units/mL catalase for 30 min.

To defend cells against oxidative stress, cells have multiple antioxidant enzymes. Mitochondrial superoxide dismutase 2

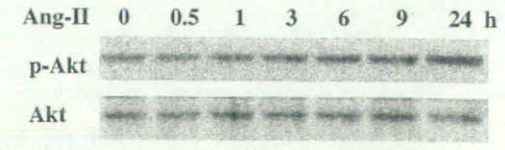

FIGURE 1. Western blots of phosphorylated Akt, total Akt, and actin. LNCaP cells cultured in steroid-free medium were harvested at the indicated times after angiotensin II (*Ang-II*; 10 μmol/L) treatment. The cells were lysed, and detergent extracts were immunoblotted with each antibody. Total protein (20 μg) was run and transferred to Immobilon-P transfer membrane and probed with phophorylated Akt and total Akt antibody.

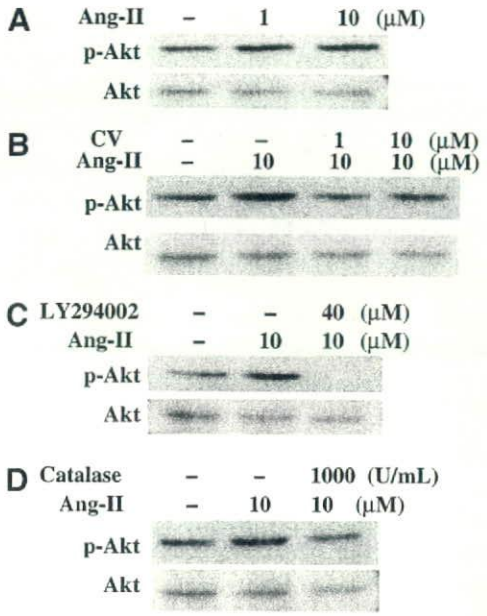

FIGURE 2. Phosphorylation of Akt induced by angiotensin II treatment and diminished by candesartan, LY294002, and catalase. **A.** LNCaP cells were stimulated with 1 or 10 μmol/L angiotensin II for 3 h. **B.** Cells were pretreated with 1 or 10 μmol/L candesartan (*CV*) for 30 min and harvested after 3 h of 10 μmol/L angiotensin II exposure. **C.** Cells were pretreated with 40 μmol/L LY294002, an inhibitor of phosphoinositide 3-kinase, for 30 min and harvested after 3 h of 10 μmol/L angiotensin II exposure. **D.** Cells were pretreated with 1,000 units/mL catalase, an antioxidant enzyme, for 30 min and harvested after 3 h of 10 μmol/L angiotensin II exposure. All Western blots of protein lysates were probed with antibodies to phosphorylated Akt (*p-Akt*) and total Akt.

(SOD2) is one of the first lines of defense. Because accumulated H_2O_2 leads to the production of hydroxyl radicals, cells are equipped with multiple enzymatic pathways for their removal. Glutathione peroxidase is one of three major pathways in the second line of defense against oxidative stress. We examined the expression of antioxidant enzymes SOD2 and glutathione peroxidase in LNCaP cells treated with 10 μmol/L angiotensin II for 24 h. As a result, the patterns of their protein expression were similar to that of p47phox expression. In brief, the expression of both antioxidant enzymes was enhanced by angiotensin II treatment for 24 h, and pretreatment with candesartan or catalase inhibited their expressions. The results of inhibition of both antioxidant enzymes by pretreatment with candesartan or catalase are convincing, because the pretreatment reduced superoxide generation associated with inhibition of p47phox.

Superoxide Anion (O_2^-) Induction by Angiotensin II Treatment

We determined the generation of the O_2^- radical, another important member of the ROS family, using fluorescent dye staining. Dihydroethidium (HE), which is a specific fluorescent dye for O_2^-, exhibits a red color after reaction with O_2^-.

After treatment with candesartan, catalase, or LY294002 for 30 min, LNCaP cells were treated with 10 μmol/L angiotensin II for 5 h. As shown in Fig. 5, angiotensin II enhanced the formation of the O_2^- radical (Fig. 5B) compared with control (Fig. 5A), whereas candesartan decreased O_2^- radical formation inside cells (Fig. 5C). Also, catalase decreased formation of the O_2^- radical induced by angiotensin II (Fig. 5D), because catalase is an antioxidant enzyme. Figure 5E shows that LY294002, an inhibitor of phosphoinositide 3-kinase, decreased the formation of the O_2^- radical induced by angiotensin II. We did semiquantitative digital image analysis of the O_2^- radical formation. Figure 5F indicates that angiotensin II enhanced the formation of the O_2^- radical ~28-fold higher than control and candesartan, catalase, and LY294002 decreased it, with which relative ratios compared with control were 0.6, 2.7, and 1.9, respectively.

To confirm whether angiotensin II enhances the formation of the O_2^- radical in prostate cancer cells, polyethylene glycol (PEG)–SOD, which is a representative antioxidant enzyme, was used as a positive control to show superoxide was being produced. Figure 6 shows that PEG-SOD clearly decreased formation of the O_2^- radical induced by angiotensin II (Fig. 6C). Semiquantitative image analysis indicates that PEG-SOD decreased O_2^- radical formation enhanced by angiotensin II at 14.2-fold down to 1.6-fold compared with control (Fig. 6D). These results provide direct evidence that angiotensin II can induce the generation of ROS in LNCaP cells and candesartan, as well as antioxidant enzymes, and an inhibitor of phosphoinositide 3-kinase can inhibit it.

Expression of Checkpoints Proteins and Measurement of 8-Hydroxy-2′-Deoxyguanosine Level

To confirm whether angiotensin II can provoke DNA damage in LNCaP cells, Western blot analyses to detect checkpoints proteins of DNA damage were done. After treatment with candesartan, catalase, or LY294002 for 30 min, LNCaP cells were treated with 10 μmol/L angiotensin II for 24 h. Figure 7A shows that angiotensin II induced the phosphorylation of p53 (Ser^{15}), Chk2 (Thr^{68}), and cdc2 (Tyr^{15}), and candesartan or catalase inhibited them. 4-Hydroxynonenal, a product of cell membrane lipid peroxidation, has been suggested to be a key mediator of oxidative stress–induced cell death (24, 25). Like the phosphorylation of checkpoint proteins, modification of proteins with 4-hydroxynonenal was enhanced by angiotensin II treatment and inhibited by candesartan or catalase (Fig. 7A). We also investigated whether androgen (dihydrotestosterone) influenced oxidative stress in LNCaP cells, which resulted in the induction of 4-hydroxynonenal by dihydrotestosterone in a dose-dependent manner (data not shown).

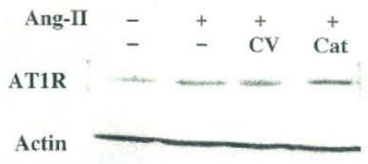

FIGURE 3. AT1 receptor expression induced by angiotensin II with/without candesartan and catalase. Western blots of AT1 receptor and actin. LNCaP cells were pretreated with 10 μmol/L candesartan or 1,000 units/mL catalase for 30 min and harvested after 24 h of 10 μmol/L angiotensin II exposure. Western blots of protein lysates were probed with anti-AT1 receptor and anti-actin antibodies.

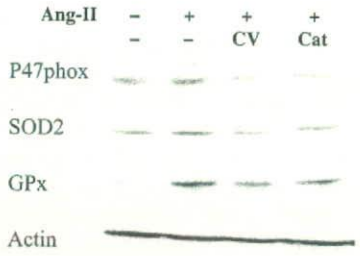

FIGURE 4. Expression of oxidative stress-related proteins induced by angiotensin II with/without candesartan and catalase. LNCaP cells were pretreated with 10 μmol/L candesartan or 1,000 units/mL catalase for 30 min and harvested after 24 h of 10 μmol/L angiotensin II exposure. Western blots of protein lysates (20 μg) were probed with antibodies to p47phox, glutathione peroxidase (*GPx*), SOD2, and actin.

As an indicator of DNA damage induced by oxidative stress, 8-hydroxy-2′-deoxyguanosine (8-OHdG) is routinely used. We examined the 8-OHdG level in the media of LNCaP cells treated with angiotensin II and/or candesartan (CV11974). The formation of 8-OHdG in LNCaP cells was significantly increased by treatment with 10 μmol/L angiotensin II (Fig. 7B) and significantly suppressed by 1 or 10 μmol/L CV11974 treatment ($P < 0.02$). These results were consistent with those of Western blots, which showed the pattern of checkpoint proteins and 4-hydroxynonenal expression induced by angiotensin II or candesartan treatment.

Inducible Nitric Oxide Synthase Expression in Prostate Cancer Cells with Angiotensin II and ARB Treatment

To confirm whether angiotensin II induces inflammation in prostate cancer cells, we did immunocyotochemical staining of an enzyme dominantly expressed during inflammatory reactions. Inducible nitric oxide synthase (iNOS) is expressed in a variety of acute or chronic inflammatory human diseases, as well as in various types of cancer, including prostate cancer (26). iNOS antibody was used to detect the expression in LNCaP cells. The secondary antibody for iNOS was Cy3, labeled and raised against rabbit IgG. LNCaP cells were stimulated with 10 μmol/L angiotensin II after treatment with two different ARBs, candesartan and telmisartan (Tel), for 30 min. After 8 h stimulation, staining of iNOS and secondary antibodies was done. Figure 8 shows that intracellular expression of iNOS was induced by stimulation with angiotensin II (Fig. 8B) compared with the control (Fig. 8A), whereas candesartan and telmisartan diminished

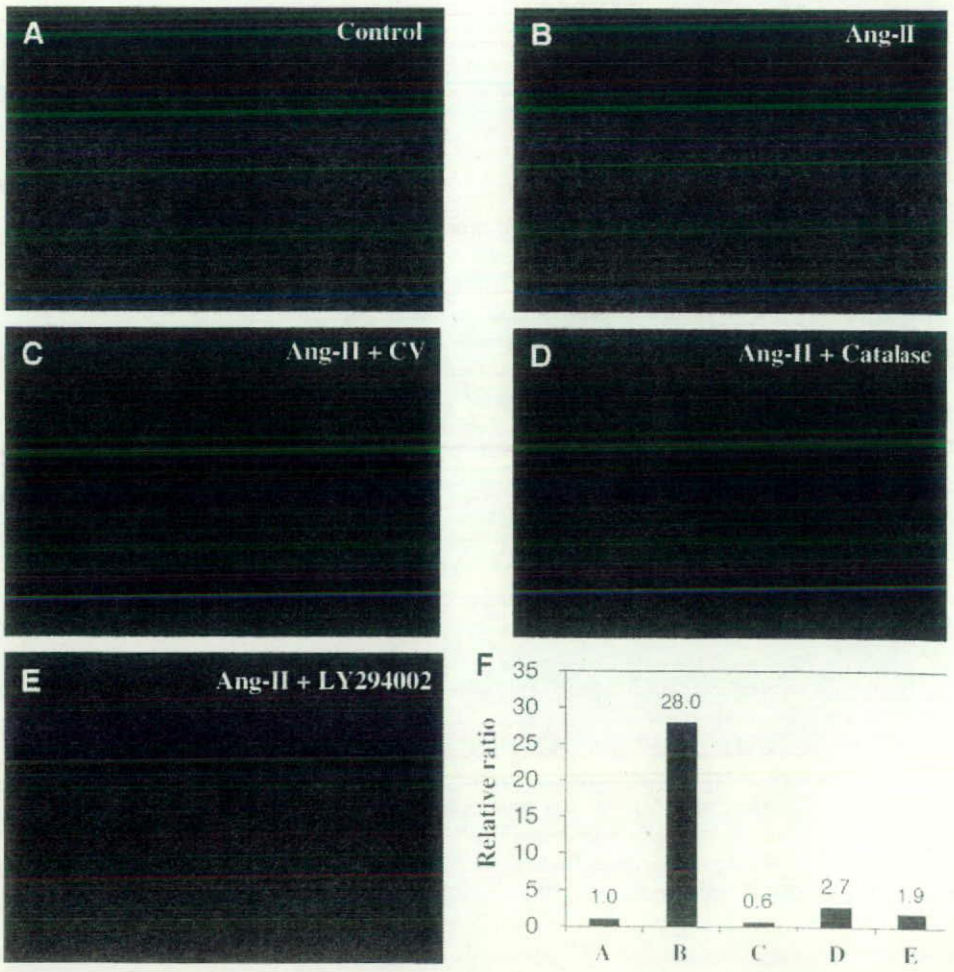

FIGURE 5. Determination of O_2^- production by H&E staining using confocal fluorescence microscope. Cells were plated onto a glass slip in a two-well plate for 24 h, followed by pretreatment with candesartan (10 μmol/L), catalase (1,000 units/mL), or LY294002 (40 μmol/L). Cells were then treated with angiotensin II (10 μmol/L) for 5 h. H&E was applied to the cells 30 min before treatment was completed. After being stained, the cells were washed twice with PBS and fixed with 10% buffered formalin. The images were captured with a confocal fluorescence microscope. **A.** Control. **B.** Angiotensin II. **C.** Angiotensin II and candesartan. **D.** Angiotensin II and catalase. **E.** Angiotensin II and LY294002. **F.** Semiquantitative digital image analysis of O_2^- production by H&E staining in each panel.

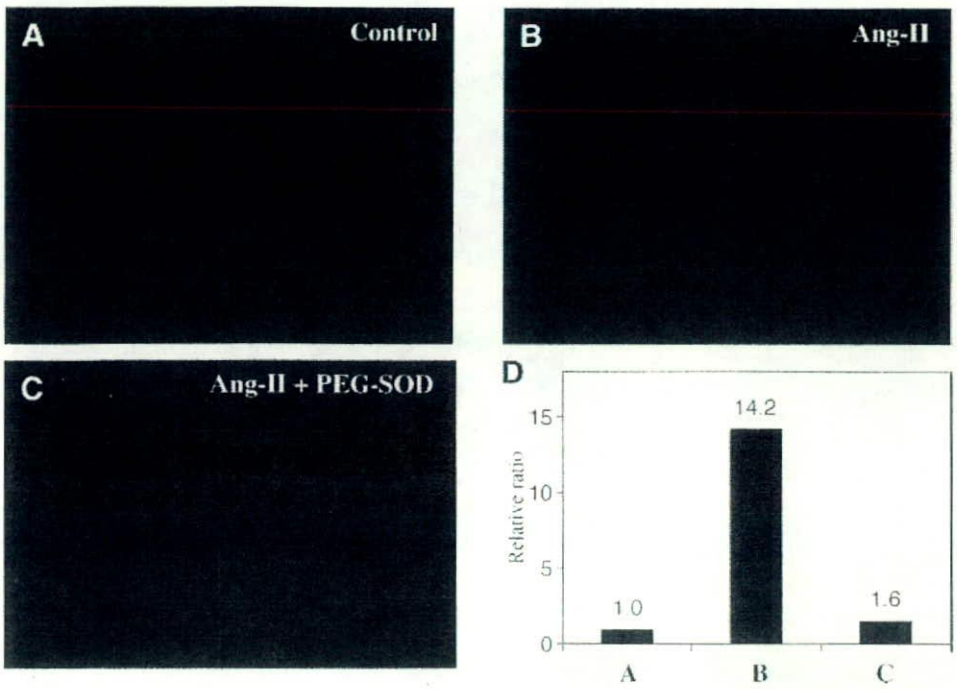

FIGURE 6. Determination of O_2^- production by H&E staining using confocal fluorescence microscope. Cells were plated onto a glass slip in a two-well plate for 24 h, followed by pretreatment with PEG-SOD (100 units/mL). Cells were then treated with angiotensin II (10 μmol/L) for 5 h. H&E was applied to the cells 30 min before treatment was completed. After being stained, the cells were washed twice with PBS and fixed with 10% buffered formalin. The images were captured with a confocal fluorescence microscope. **A.** Control. **B.** Angiotensin II. **C.** Angiotensin II and PEG-SOD. **D.** Semiquantitative digital image analysis of O_2^- production by H&E staining in each panel.

iNOS expression induced by angiotensin II (Fig. 8C and D). Like in LNCaP cells, similar phenomena were shown in DU145 cells (data not shown).

Discussion

Although angiotensin II is well known to be an important factor in hypertension, it has also been reported to play a central role in proliferation and/or differentiation in specific organs, linking it to the progression of cancer (13, 14). Previously, we have reported that angiotensin II facilitates the secretion of some growth factors and cytokines from prostate stromal cells, resulting in cell proliferation of prostate cancer (16). Given that angiotensin II induces oxidative stress in vascular cells, it is very interesting to speculate that angiotensin II may function as an inducer of oxidative stress implicated in carcinogenesis. In the present study, we examined whether angiotensin II has the potential to evoke oxidative stress in prostate cancer cells. The expression of SOD2, one of the mitochondrial antioxidant enzymes, was time-dependently enhanced by angiotensin II treatment in prostate cancer cells (data not shown). Also, angiotensin II induced the expression of p47phox, one of cytosolic NADPH oxidases, whereas the angiotensin receptor blocker candesartan (CV11974) inhibited its expression in prostate cancer cells. Furthermore, angiotensin II induced the expression of antioxidant enzymes, glutathione peroxidase, and SOD2, and candesartan inhibited their expression. It is well known that oxidative stress induces DNA and protein adducts, and similarly, angiotensin II induced the expression of 8-OHdG and modification of protein with 4-hydroxynonenal expression in prostate cancer cells.

Early reports revealed the existence of RAS in the prostate; all components of RAS, including angiotensinogen, renin, ACE, and angiotensin receptors (27-31), have been identified in the prostate. Intriguingly, a 3-fold to 5-fold higher concentration of angiotensin II was confirmed in seminal fluid in comparison with that in blood (32), which strongly supports the existence of RAS in the prostate gland. Likewise, it was reported that there was a high concentration of angiotensin II in pancreatic cancer tissue compared with that in normal tissue (33), and RAS components, including angiotensinogen, angiotensin II receptor type 1, and renin, have been identified in the islets of Langerhans (34). These findings provide supportive evidence that the local RAS in these organs, especially angiotensin II, may exert paracrine effects in the development of prostate and pancreatic cancer. The possible mechanism of carcinogenesis by angiotensin II is expected to be induction of oxidative stress in these organs.

We previously clarified that angiotensin II acted as a growth factor in prostate cancer and stromal cells (14, 16). Interestingly, earlier investigators have reported that angiotensin II induced oxidative stress in vascular cells, for example, demonstrating that angiotensin II stimulated the production of ROS in endothelial cells by up-regulating the subunits of NADPH oxidases (17, 18). In the present study, we confirmed that angiotensin II–induced production of the O_2^- radical in prostate cancer cells, as shown in Fig. 5. Higashi et al. confirmed that NADPH oxidase is the most important source of ROS in the vasculature (35). It is well known that NAPDH oxidase is composed of cytosolic components, such as p47phox, p67phox, and RC1, and membrane-spanning components, such as p22phox and gp91phox. Angiotensin II–induced NADPH oxidase activation is one of the major sources of ROS in the pathophysiologic mechanism of atherosclerosis (35, 36). These observations are consistent with the findings of the present study, in which angiotensin II induced the expression of p47phox and production of the O_2^- radical.

It is likely that induction of ROS subjects the cell to a state of oxidative stress, leading to damage of cellular DNA and proteins (37). A growing body of evidence has shown that excessive lipid peroxidation generated by oxidative stress may be involved in carcinogenesis. Especially, 4-hydroxynonenal is a major product of lipid peroxidation, and its level becomes relatively high in cells under oxidative stress (38). An augmented level of 4-hydroxynonenal was observed in oxidative stress-related degenerative diseases (39, 40). Furthermore, accumulation of 8-OHdG has been shown to lead to G:C-to-T:A transversion mutations that are prevalent in mutated oncogenes and tumor suppressor genes (41, 42). As shown in the present data, angiotensin II stimulation augmented DNA and protein markers, such as 8-OHdG, in prostate cancer cells. In general, DNA damage triggers the cell cycle checkpoints G_2-M and G_1-S through activation of kinases, e.g., phosphorylation of Chk2 at Thr^{68} and multiple sites in p53 (43, 44). Our data also showed that angiotensin II induced the phosphorylation of Chk2 (Tbr^{68}) and p53 (Ser^{15}). Chronic oxidative stress has been implicated in neoplastic transformation (45) and promotion of tumorigenesis (46). The present study provides evidence that ROS generated by angiotensin II may contribute to DNA damage and be involved in carcinogenesis of the prostate gland.

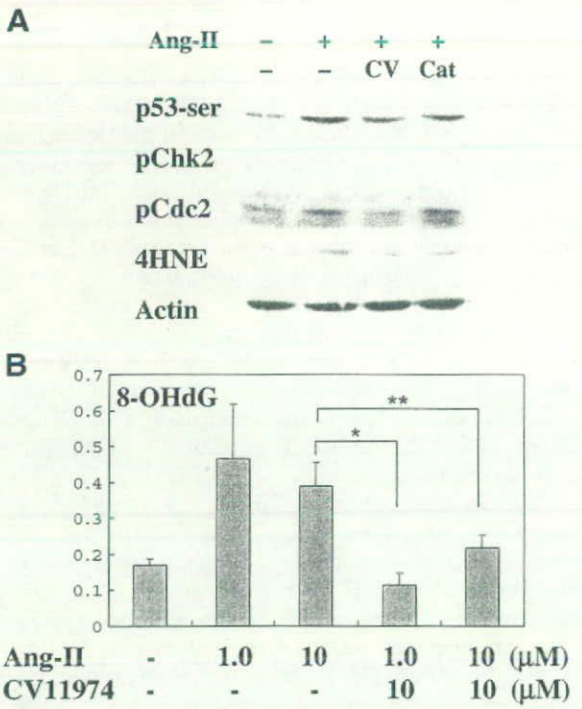

FIGURE 7. DNA damage in LNCaP cells by angiotensin II treatment. **A.** LNCaP cells were pretreated with 10 μmol/L candesartan or 1,000 units/mL catalase for 30 min and harvested after 24 h of 10 μmol/L angiotensin II exposure. Western blots of protein lysates (20 μg) were probed with antibodies to checkpoint proteins, including phosphorylated p53 (Ser^{15}), phosphorylated Chk2 (Thr^{68}), phosphorylated cdc2 (Tyr^{15}), and actin. To examine the DNA damage by angiotensin II treatment, Western blot was also done using anti–4-hydroxynonenal (*4HNE*) antibody. **B.** 8-OHdG level was measured after treatment with angiotensin II at the indicated concentrations or simultaneously with 10 μmol/L candesartan (CV11974). Columns, mean of three different experiments; bars, SD. Candesartan (CV11974) treatment significantly suppressed 8-OHdG level induced by 1 or 10 μmol/L CV11974 treatment (* or **, $P < 0.05$).

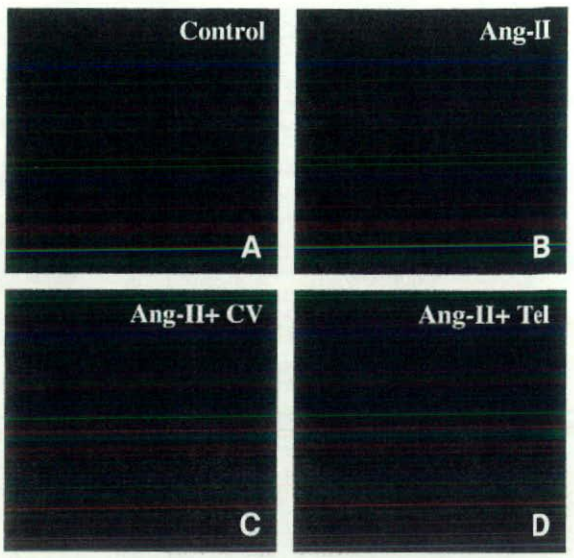

FIGURE 8. Immunocytochemical staining of iNOS in LNCaP cells. Intracellular expression of iNOS was induced by stimulation with 10 μmol/L angiotensin II (**B**) compared with the control (**A**), whereas 10 μmol/L CV11974 and 1 μmol/L telmisartan, an ARB, diminished iNOS expression induced by angiotensin II treatment (**C** and **D**).

The present data showing that angiotensin II enhanced iNOS expression and ARBs inhibited it in prostate cancer cells support the evidence that angiotensin II is a peptide involved in inflammation. In vascular smooth muscle cells, iNOS may be induced by various cytokines, including interleukin 1β, tumor necrosis factor α, IFN-γ, and interleukin 6 (47). Also, iNOS was strongly observed in inflamed epithelium. Earlier studies have shown that iNOS is expressed in epithelial cells in patients with colitis who are prone to colon cancer (48-50). Regarding the link between iNOS and cancer development, the expression of iNOS was higher in cancer specimens than in normal tissue in esophageal, colon, and thyroid carcinomas (51, 52). Baltaci et al. reported that the expression of iNOS was higher in high-grade PIN and prostatic carcinoma samples than in benign prostatic hypertrophy and low-grade PIN samples. These findings suggest that nitric oxide produced by iNOS may be involved in prostate tumorigenesis (53). In addition, Calvisi et al. revealed that iNOS and NADPH oxidase were involved in ROS generation during c-Myc/transforming growth factor α hepatocarcinogenesis and were inhibited by antioxidant agent treatment (54).

There have recently been several reports suggesting a relationship between chronic inflammation and prostate cancer. It is plausible that ROS released by inflammatory cells during cycles of cellular damage and regeneration in the organ result in permanent DNA damage (55). The prostate gland is a common site of chronic inflammation. Although most focal lesions of prostatic atrophy are considered quiescent, prostate epithelial cell proliferation is increased in some lesions, and thus, focal prostatic atrophy, which is associated with chronic inflammation, is considered to be proliferative (56).

Pathologic findings support the hypothesis that chronic inflammation may be involved in prostate cancer development. Novel observations have been reported regarding the pathologic entity of focal prostatic epithelial atrophy (57), which is associated with chronic inflammation with proliferative change, designated "proliferative inflammatory atrophy." More interestingly, these areas are commonly adjacent to high-grade PIN or local foci of cancer in the prostate of older men (58). Proliferative inflammatory atrophy lesions have been regarded as a precursor lesion of prostate cancer (59). In an experimental study, prostatic tissue with inflammation caused by bacterial infection showed atypical hyperplasia and areas of dysplasia showed stronger staining for oxidative DNA damage and greater epithelial cell proliferation than normal prostatic gland (60). The pathogenesis of the development of prostate cancer possibly involves ROS generated through various actions of androgen, infection, or angiotensin II, as mentioned above. Theoretically, it is proposed that long-term exposure to ROS may cause DNA and protein damage, cell proliferation, and enhancement of oncogenes, linking it to the development of proliferative inflammatory atrophy, PIN, and, finally, prostate cancer (Fig. 9).

Androgen is also likely to play a central role in prostate carcinogenesis. There has been increasing evidence to support the hypothesis that oxidative stress induced by androgen, at least in part, contributes to carcinogenesis. Androgen-induced ROS may directly or indirectly result from its influence on mitochondria (61). An *in vitro* study using androgen-sensitive human prostate cancer cells, LNCaP, showed that stimulation with a physiologic level of androgen resulted in an increased level of ROS (62). Supporting this hypothesis, Sun et al. suggested that prostate-specific antigen, a representative androgen-dependent protein, markedly stimulates the generation of ROS in LNCaP cells. They also showed that the effect of testosterone on ROS was suppressed by flutamide and by anti–prostate-specific antigen antibody (63).

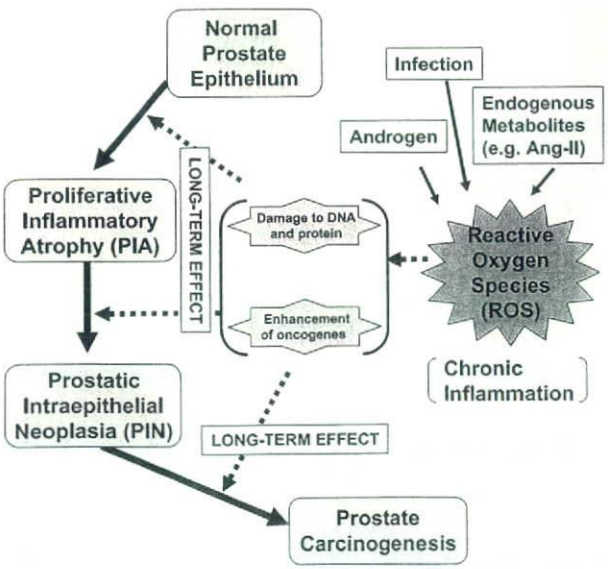

FIGURE 9. Pathogenesis of prostate cancer possibly involves ROS generated by various actions of androgen, infection, or angiotensin II. Theoretically, it is proposed that long-term exposure to ROS causes DNA and protein damage, cell proliferation, and enhancement of oncogenes, linking it to the formation of proliferative inflammatory atrophy (*PIA*), PIN, and, finally, prostate cancer.

In conclusion, epidemiologic, experimental, and clinical studies have implicated oxidative stress in the development and progression of prostate cancer. The present study indicated that oxidative stress caused by the local generation of angiotensin II may be involved in the development of prostate cancer. A greater understanding of the molecular events associated with oxidative stress will contribute to better strategies for the chemoprevention of prostate cancer.

Materials and Methods

Cell Lines

LNCaP cells, a human prostate cancer cell line, were obtained from the American Type Culture Collection. LNCaP cells were cultured in F-12 medium supplemented with 10% FCS under 5% CO_2 before the experiments. In the experiments, LNCaP cells were cultured in phenol red–free RPMI plus 0.1% bovine serum albumin and stimulated with reagents. Cells were used for each experiment within 10 to 12 passages.

Reagents

Angiotensin II was purchased from Auspep Pty. Anti-SOD2 antibody was purchased from Millipore. Anti-p47phox, anti-AT1 receptor, and anti-iNOS antibodies were purchased from Santa Cruz Biotechnology. Anti–4-hydroxynonenal antibody was purchased from NOF Co. Anti-Akt, phosphorylated Akt, phosphorylated p53 (Ser^{15}), phosphorylated Chk2 (Thr^{68}), and phosphorylated cdc2 (Tyr^{15}) antibodies were purchased from Cell Signaling Technology. Catalase, PEG-SOD, and LY294002 were purchased from Sigma. The ARBs candesartan (CV11974) and telmisartan were provided by Takeda Pharmaceutical Co. and Boehringer Ingelheim, respectively.

Immunocytochemical Staining

Cells plated on culture slides, Lab-Tek Chamber Slide (Nalge Nunc International), were rinsed with PBS twice before they were fixed in 2% paraformaldehyde/PBS at room temperature for 15 min. Fixed cells were washed with 100 mmol/L ammonium chloride for 10 min and permeabilized with 0.1% Triton X-100/PBS for 10 min. These cells were blocked with 10% normal goat serum/PBS for 1 h. Primary antibody against iNOS was diluted 1:100 in 10% normal goat serum/TBST [20 mmol/L Tris-HCl (pH 8.0), 150 mmol/L NaCl, 0.05% Tween 20] and applied for 1 h in a 37°C chamber. After an additional three washes with TBST for 5 min, cells were incubated with Cy3-labeled secondary antibody for 1 h in a 37°C chamber. Before cells were mounted in antifade reagent, they were washed thrice in TBST for 5 min. As a control, sections were incubated without treatment with angiotensin II or nonprimary antibody. Images were captured using a fluorescence microscope (BZ-8000; Keyence).

Superoxide Anion (O_2^-) Assay

Dihydroethidium (HE), which is a specific dye for O_2^-, is oxidized by O_2^- to ethidium, which stains the nucleus a bright

fluorescent red. The cells were plated onto a glass slip in a two-well plate at 2×10^5 cells per well and incubated for 24 h. Cells were then treated with 10 μmol/L angiotensin II for 5 h after pretreatment with candesartan, catalase, or LY294002 for 30 min. HE was added into the cell culture 30 min before treatment was completed. After being stained, the cells were washed in cold 1 × PBS and fixed with 10% buffered formalin. The slip was mounted on a glass slide and observed using a fluorescence microscope (BZ-8000, Keyence) fitted with an argon-ion laser.

Semiquantitative Digital Image Analysis

To quantify the levels of O_2^- production, we used Image J (NIH) to perform semiquantitative digital image analysis of H&E staining. The panels of Figs. 5 and 6 were split into red and blue images, and the mean level values of red and blue images were measured. The levels of O_2^- production were determined by dividing the mean level of red by that of blue in each panel.

Determination of 8-OHdG Level

LNCaP and DU145 cells were cultured on culture slides in phenol red–free RPMI plus 0.1% bovine serum albumin for 24 h, and the medium was collected immediately at 24 h after 10 μmol/L angiotensin II exposure with/without 10 μmol/L CV11974 or 1 μmol/L telmisartan as indicated in the figures. 8-OHdG level was measured as previously reported, according to the manufacturer's instructions (64). In brief, culture supernatants after these treatments as described above were centrifuged at 10,000 × *g* for 10 min, and the supernatants were used for the determination of 8-OHdG level using a quantitative sandwich ELISA kit (NOF Co.) with a determination range of 0.125 to 10 ng/mL. Absorbance was determined with a microplate reader (Bio-Rad) at 450 nm. All analyses and calibrations were done in triplicate. A standard curve was created using Excel (Microsoft 2003 version) by plotting the logarithm of the mean absorbance of each sample versus the sample concentration.

Western Blot Analysis

LNCaP cells were cultured in phenol red–free RPMI plus 0.1% bovine serum albumin for 24 h. Then cells were pretreated with 10 μmol/L CV11974, 1,000 units/mL catalase, or 40 μmol/L LY294002 for 30 min and harvested at several points as indicated in the figures after 10 μmol/L angiotensin II exposure. Cells in the appropriate conditions were washed twice with ice-cold PBS, lysed in ice-cold buffer consisting of 20 mmol/L Tris (pH 8.0), 137 mmol/L NaCl, 10% glycerol, 0.1% SDS, 0.5% Nonidet P-40, 100 mmol/L sodium fluoride, 200 mmol/L sodium orthovanadate, 1 mmol/L EGTA, 2 mmol/L phenylmethylsulfonyl fluoride, 1 mg/mL leupeptin, and 3 mg/mL aprotinin, and centrifuged (30 min, 4°C, 14,500 × *g*). After quantitation, 20 μg of each cell lysate were added to SDS gel loading buffer (containing a reducing agent) and boiled for 5 min. The samples were subjected to SDS-PAGE on 10% gel and electrotransferred to Immobilon-P (Millipore). After blocking the membrane with 5% albumin, Western blotting was done using the antibody of interest, and the product was detected with an enhanced chemiluminescence detection system (Amersham).

Statistical Analysis

Significance was examined by ANOVA followed by *t* test, and differences with $P < 0.05$ (*) were considered significant.

References

1. Jemal A, Thomas A, Murray T, Thun M. Cancer statistics, 2002. CA Cancer J Clin 2002;52:23–47.

2. Fujinami K, Uemura H, Ishiguro H, Kubota Y. Liprin-α2 gene, protein tyrosine phosphatase LAR interacting protein related gene, is downregulated by androgens in the human prostate cancer cell line LNCaP. Int J Mol Med 2002;10:173–6.

3. Ishiguro H, Uemura H, Fujinami K, Ikeda N, Ohta S, Kubota Y. 55 kDa nuclear matrix protein (nmt55) mRNA is expressed in human prostate cancer tissue and is associated with the androgen receptor. Int J Cancer 2003;105:26–32.

4. Hasumi H, Ishiguro H, Nakamura M, et al. Neuroserpin (PI-12) is upregulated in high-grade prostate cancer and is associated with survival. Int J Cancer 2005;115:911–6.

5. Smith GR, Missailidis S. Cancer, inflammation and the AT1 and AT2 receptors. J Inflamm Lond 2004;1:3.

6. Hussain SP, Hofseth LJ, Harris CC. Radical causes of cancer. Nat Rev Cancer 2003;3:276–85.

7. Coussens LM, Werb Z. Inflammation and cancer. Nature 2002;420:860–7.

8. Baker AM, Oberley LW, Cohen MB. Expression of antioxidant enzymes in human prostatic adenocarcinoma. Prostate 1997;32:229–33.

9. Chang F, Lee JT, Navolanic PM, et al. Involvement of PI3K/Akt pathway in cell cycle progression, apoptosis, and neoplastic transformation: a target for cancer chemotherapy. Leukemia 2003;17:590–603.

10. Lee WH, Morton RA, Epstein JI, et al. Cytidine methylation of regulatory sequences near the pi-class glutathione S-transferase gene accompanies human prostatic carcinogenesis. Proc Natl Acad Sci U S A 1994;91:11733–7.

11. Lim SD, Sun C, Lambeth JD, et al. Increased Nox1 and hydrogen peroxide in prostate cancer. Prostate 2005;62:200–7.

12. Wang J, Torbenson M, Wang Q, Ro JY, Becich M. Expression of inducible nitric oxide synthase in paired neoplastic and non-neoplastic primary prostate cell cultures and prostatectomy specimen. Urol Oncol 2003;21:117–22.

13. Fujimoto Y, Sasaki T, Tsuchida A, Chayama K. Angiotensin II type 1 receptor expression in human pancreatic cancer and growth inhibition by angiotensin II type 1 receptor antagonist. FEBS Lett 2001;495:197–200.

14. Uemura H, Ishiguro H, Nakaigawa N, et al. Angiotensin II receptor blocker shows antiproliferative activity in prostate cancer cells: a possibility of tyrosine kinase inhibitor of growth factor. Mol Cancer Ther 2003;2:1139–47.

15. Uemura H, Nakaigawa N, Ishiguro H, Kubota Y. Antiproliferative efficacy of angiotensin II receptor blockers in prostate cancer. Curr Cancer Drug Targets 2005;5:307–23.

16. Uemura H, Ishiguro H, Nagashima Y, et al. Antiproliferative activity of angiotensin II receptor blocker through cross-talk between stromal and epithelial prostate cancer cells. Mol Cancer Ther 2005;4:1699–709.

17. Rueckschloss U, Quinn MT, Holtz J, Morawietz H. Dose-dependent regulation of NAD(P)H oxidase expression by angiotensin II in human endothelial cells: protective effect of angiotensin II type 1 receptor blockade in patients with coronary artery disease. Arterioscler Thromb Vasc Biol 2002;22:1845–51.

18. Landmesser U, Cai H, Dikalov S, et al. Harrison DG, Role of p47(phox) in vascular oxidative stress and hypertension caused by angiotensin II. Hypertension 2002;40:511–5.

19. O'Mahony OA, Djahanbahkch O, Mahmood T, Puddefoot JR, Vinson GP. Angiotensin II in human seminal fluid. Hum Reprod 2000;15:1345–9.

20. Grove KL, Speth RC, Senger PL. Angiotensin II as a semen extender component increases retention of spermatozoa within the uterus of the heifer. Reprod Fertil Dev 1997;9:545–9.

21. Holbro T, Beerli RR, Maurer F, Koziczak M, Barbas CF III, Hynes NE. The ErbB2/ErbB3 heterodimer functions as an oncogenic unit: ErbB2 requires ErbB3 to drive breast tumor cell proliferation. Proc Natl Acad Sci U S A 2003;100:8933–8.

22. Shelton JG, Steelman LS, Lee JT, et al. Effects of the RAF/MEK/ERK and PI3K/AKT signal transduction pathways on the abrogation of cytokine-dependence and prevention of apoptosis in hematopoietic cells. Oncogene 2003;22:2478–92.

23. Santos SC, Lacronique V, Bouchaert I, et al. Constitutively active STAT5 variants induce growth and survival of hematopoietic cells through a PI 3-kinase/Akt dependent pathway. Oncogene 2001;20:2080–90.

24. Poli G, Schaur RJ. 4-Hydroxynonenal in the pathomechanisms of oxidative stress. IUBMB Life 2000;50:315–21.

25. Nakashima I, Liu W, Akhand AA, et al. 4-Hydroxynonenal triggers multistep signal transduction cascades for suppression of cellular functions. Mol Aspects Med 2003;24:231–8.

26. Kroncke KD, Suschek CV, Kolb-Bachofen V. Implications of inducible nitric oxide synthase expression and enzyme activity. Antioxid Redox Signal 2000;2: 585–605.

27. Dinh DT, Frauman AG, Somers GR, et al. Evidence for activation of the renin-angiotensin system in the human prostate: increased angiotensin II and reduced AT(1) receptor expression in benign prostatic hyperplasia. J Pathol 2002; 196:213–9.

28. Nassis L, Frauman AG, Ohishi M, et al. Localization of angiotensin-converting enzyme in the human prostate: pathological expression in benign prostatic hyperplasia. J Pathol 2001;195:571–9.

29. Dinh DT, Frauman AG, Casley DJ, Johnston CI, Fabiani ME. Angiotensin AT(4) receptors in the normal human prostate and benign prostatic hyperplasia. Mol Cell Endocrinol 2001;184:187–92.

30. Dinh DT, Frauman AG, Sourial M, Casley DJ, Johnston CI, Fabiani ME. Identification, distribution, and expression of angiotensin II receptors in the normal human prostate and benign prostatic hyperplasia. Endocrinology 2001; 142:1349–56.

31. Fabiani ME, Sourial M, Thomas WG, Johnston CI, Johnston CI, Frauman AG. Angiotensin II enhances noradrenaline release from sympathetic nerves of the rat prostate via a novel angiotensin receptor: implications for the pathophysiology of benign prostatic hyperplasia. J Endocrinol 2001;171:97–108.

32. O'Mahony OA, Barker S, Puddefoot JR, Vinson GP. Synthesis and secretion of angiotensin II by the prostate gland *in vitro*. Endocrinology 2005;146:392–8.

33. Ohta T, Amaya K, Yi S, et al. Angiotensin converting enzyme-independent, local angiotensin II-generation in human pancreatic ductal cancer tissues. Int J Oncol 2003;23:593–8.

34. Tahmasebi M, Puddefoot JR, Inwang ER, Vinson GP. The tissue renin-angiotensin system in human pancreas. J Endocrinol 1999;161:317–22.

35. Higashi Y, Chayama K, Yoshizumi M. Angiotensin II type I receptor blocker and endothelial function in humans: role of nitric oxide and oxidative stress. Curr Med Chem Cardiovasc Hematol Agents 2005;3:133–48.

36. Dzau VJ. Theodore Cooper Lecture: tissue angiotensin and pathobiology of vascular disease: a unifying hypothesis. Hypertension 2001;37:1047–52.

37. Martindale JL, Holbrook NJ. Cellular response to oxidative stress: signaling for suicide and survival. J Cell Physiol 2002;192:1–15.

38. Feng Z, Hu W, Tang MS. Trans-4-hydroxy-2-nonenal inhibits nucleotide excision repair in human cells: a possible mechanism for lipid peroxidation-induced carcinogenesis. Proc Natl Acad Sci U S A 2004;101:8598–602.

39. Soh Y, Jeong KS, Lee IJ, Bae MA, Kim YC, Song BJ. Selective activation of the c-Jun N-terminal protein kinase pathway during 4-hydroxynonenal-induced apoptosis of PC12 cells. Mol Pharmacol 2000;58:535–41.

40. Romero FJ, Bosch-Morell F, Romero MJ, et al. Lipid peroxidation products and antioxidants in human disease. Environ Health Perspect 1998;106 Suppl 5: 1229–34.

41. Shibutani S, Takeshita M, Grollman AP. Insertion of specific bases during DNA synthesis past the oxidation-damaged base 8-oxodG. Nature 1991;349: 431–4.

42. Hussain SP, Harris CC. Molecular epidemiology of human cancer: contribution of mutation spectra studies of tumor suppressor genes. Cancer Res 1998;58:4023–37.

43. Matsuoka S, Rotman G, Ogawa A, Shiloh Y, Tamai K, Elledge SJ. Ataxia telangiectasia-mutated phosphorylates Chk2 *in vivo* and *in vitro*. Proc Natl Acad Sci U S A 2000;97:10389–94.

44. Tibbetts RS, Brumbaugh KM, Williams JM, et al. A role for ATR in the DNA damage-induced phosphorylation of p53. Genes Dev 1999;13:152–7.

45. Suh YA, Arnold RS, Lassegue B, et al. Cell transformation by the superoxide-generating oxidase Mox1. Nature 1999;401:79–82.

46. Arbiser JL, Petros J, Klafter R, et al. Reactive oxygen generated by Nox1 triggers the angiogenic switch. Proc Natl Acad Sci U S A 2002;99:715–20.

47. de Vera ME, Shapiro RA, Nussler AK, et al. Transcriptional regulation of human inducible nitric oxide synthase (NOS2) gene by cytokines: initial analysis of the human NOS2 promoter. Proc Natl Acad Sci U S A 1996;93: 1054–9.

48. Wiseman H, Halliwell B. Damage to DNA by reactive oxygen and nitrogen species: role in inflammatory disease and progression to cancer. Biochem J 1996; 313:17–29.

49. Hofseth LJ, Saito S, Hussain SP, et al. Nitric oxide-induced cellular stress and p53 activation in chronic inflammation. Proc Natl Acad Sci U S A 2003;100: 143–8.

50. Singer II, Kawka DW, Scott S, et al. Expression of inducible nitric oxide synthase and nitrotyrosine in colonic epithelium in inflammatory bowel disease. Gastroenterology 1996;111:871–85.

51. Kojima M, Morisaki T, Tsukahara Y, et al. Nitric oxide synthase expression and nitric oxide production in human colon carcinoma tissue. J Surg Oncol 1999; 70:222–9.

52. Kitano H, Kitanishi T, Nakanishi Y, et al. Expression of inducible nitric oxide synthase in human thyroid papillary carcinomas. Thyroid 1999;9:113–7.

53. Baltaci S, Orhan D, Gogus C, Turkolmez K, Tulunay O, Gogus O. Inducible nitric oxide synthase expression in benign prostatic hyperplasia, low- and high-grade prostatic intraepithelial neoplasia and prostatic carcinoma. BJU Int 2001;88: 100–3.

54. Calvisi DF, Ladu S, Hironaka K, Factor VM, Thorgeirsson SS. Vitamin E down-modulates iNOS and NADPH oxidase in c-Myc/TGF-α transgenic mouse model of liver cancer. J Hepatol 2004;41:815–22.

55. Ames BN. Mutagenesis and carcinogenesis: endogenous and exogenous factors. Environ Mol Mutagen 1989;14 Suppl 16:66–77.

56. Ruska KM, Sauvageot J, Epstein JI. Histology and cellular kinetics of prostatic atrophy. Am J Surg Pathol 1998;22:1073–7.

57. Rich AR. Classics in oncology. On the frequency of occurrence of occult carcinoma of the prostate: Arnold Rice Rich MD, Journal of Urology 33:3, 1935. CA Cancer J Clin 1979;29:115–9.

58. Nakayama M, Bennett CJ, Hicks JL, et al. Hypermethylation of the human glutathione S-transferase-pi gene (GSTP1) CpG island is present in a subset of proliferative inflammatory atrophy lesions but not in normal or hyperplastic epithelium of the prostate: a detailed study using laser-capture microdissection. Am J Pathol 2003;163:923–33.

59. Palapattu GS, Sutcliffe S, Bastian PJ, et al. Prostate carcinogenesis and inflammation: emerging insights. Carcinogenesis 2005;26:1170–81.

60. Elkahwaji JE, Zhong W, Hopkins WJ, Bushman W. Chronic bacterial infection and inflammation incite reactive hyperplasia in a mouse model of chronic prostatitis. Prostate 2007;67:14–21.

61. Ripple MO, Hagopian K, Oberley TD, Schatten H, Weindruch R. Androgen-induced oxidative stress in human LNCaP prostate cancer cells is associated with multiple mitochondrial modifications. Antioxid Redox Signal 1999;1:71–81.

62. Ripple MO, Henry WF, Rago RP, Wilding G. Prooxidant-antioxidant shift induced by androgen treatment of human prostate carcinoma cells. J Natl Cancer Inst 1997;89:40–8.

63. Sun XY, Donald SP, Phang JM. Testosterone and prostate specific antigen stimulate generation of reactive oxygen species in prostate cancer cells. Carcinogenesis 2001;22:1775–80.

64. Miyake H, Hara I, Gleave ME, Eto H. Protection of androgen-dependent human prostate cancer cells from oxidative stress-induced DNA damage by overexpression of clusterin and its modulation by androgen. Prostate 2004;61: 318–23.

RESEARCH COMMUNICATION

Suppression of Prostate Cancer Growth by Resveratrol in The Transgenic Rat for Adenocarcinoma of Prostate (TRAP) Model

Azman Seeni, Satoru Takahashi*, Kentaro Takeshita, Mingxi Tang, Satoshi Sugiura, Shin-ya Sato, Tomoyuki Shirai

Abstract

Research into actions of resveratrol, abundantly present in red grape skin, has been greatly stimulated by its reported beneficial health influence. Since it was recently proposed as a potential prostate cancer chemopreventive agent, we here performed an in vivo experiment to explore its effect in the Transgenic Rat for Adenocarcinoma of Prostate (TRAP) model, featuring the rat probasin promoter/SV 40 T antigen. Resveratrol suppressed prostate cancer growth and induction of apoptosis through androgen receptor (AR) down-regulation, without any sign of toxicity. Resveratrol not only downregulated androgen receptor (AR) expression but also suppressed the androgen responsive glandular kallikrein 11 (Gk11), known to be an ortholog of the human prostate specific antigen (PSA), at the mRNA level. The data provide a mechanistic basis for resveratrol chemopreventive efficacy against prostate cancer.

Key Words: Chemoprevention - prostate cancer - resveratrol - TRAP rats

-Asian Pacific J Cancer Prev, 9, 7-14

Introduction

Prostate cancer has become the most frequently diagnosed cancer and the second leading cause of cancer-related death for men in the United States (Jemal et al., 2007). The conventional treatments available for this disease, such as hormone therapy, chemotherapy or radical prostatectomy, eventually fail to exert control and metastatic disease frequently develops even after surgery and may cause death. Therefore, interest has focused on chemoprevention, suppressing, delaying or reversing carcinogenesis by pharmacologic intervention with naturally occurring or synthetic agents (Sporn and Suh, 2002;Tsao et al., 2004).

Resveratrol, a phytoestrogen, found in grapes and red wine, has been identified as a novel potential cancer chemopreventive agent. Numerous reviews have been published regarding its activity (Jang et al., 1997;Bhat and Pezzuto, 2002; Stewart et al., 2003; Aziz et al., 2003; Aggarwal et al., 2004; Baur and Sinclair, 2006; Delmas et al., 2006) but the molecular mechanisms have yet to be fully defined, especially *in vivo*. Therefore, we explored the effects of resveratrol using the Transgenic Rat for Adenocarcinoma of Prostate (TRAP) model, established in our laboratory using the Simian virus 40 T antigen under control of the probasin gene promoter (Asamoto et al., 2001a; Asamoto et al., 2002). The animals develop high grade prostatic intraepithelial neoplasia (PIN) and well differentiated adenocarcinoma with high incidence in all prostate lobes at 15 weeks of age, all lesions being completely androgen-dependent. The model provides an ideal tool to gain insights into possible mechanisms for prostate cancer prevention (Asamoto et al., 2001b; Cho et al., 2003; Zeng et al., 2005; Kandori et al., 2005; Said et al., 2006; Tang et al., 2007) in the relatively short-term. To our knowledge, the present study provided the first evidence that resveratrol inhibits prostate carcinogenesis in a rat model closely mimicking the human disease. The clues obtained as to the molecular basis of action are of critical importance as the first steps towards human clinical trials.

Materials and Methods

Animals

Male heterozygous TRAP rats were housed three per plastic cage on wood-chip bedding in an air conditioned specific pathogen free (SPF) animal room under standard conditions with food (Oriental MF, Oriental Yeast, Tokyo, Japan) and water *ad libitum*. All animal experiments were performed under protocols approved by the Institutional Animal Care and Use Committee of Nagoya City University Graduate School of Medical Sciences.

Chemicals, reagents and cell lines

Resveratrol was purchased from Sigma, and MG132 and cycloheximide from Calbiochem (EMD Biosciences, Inc., San Diego, CA). Antibodies to cleaved caspase 3, 7, Erk1/2 and phospho-Erk1/2 were purchased from Cell Signaling Technology (Beverly, MA). Anti-AR antibody (PG-21) was from Upstate Technology (Lake Placid, NY), anti-HA-Tag antibody was from BD Sciences Clontech

*Department of Experimental Pathology and Tumor Biology, Nagoya City University Graduate School of Medical Sciences, Nagoya, 467-8601, Japan. *For Correspondence : E-mail: sattak@med.nagoya-cu.ac.jp FAX: +81-52-842-0817*

(Palo Alto, CA), anti-cyclin D1 was from Oncogene Research Product, anti-Bcl-xL was from Pharmingen, anti-SV40T Ag was from Santa Cruz Biotechnology Inc. and anti-β-actin was from Sigma. COS7 and LNCaP were from the American Type Culture Collection (Manassas, VA). PLS30 cells were established in our laboratory as described previously (Nakanishi et al., 1996; Kato et al., 1998).

Plasmids

To generate pBKCMV-rAR, the rat AR open reading frame (ORF) was amplified by PCR and inserted into pBKCMV (Stratagene). For pGL3-rPBP-luc, a rat probasin promoter fragment (-426 ~ +32) was amplified and inserted into pGL3-basic (Promega). HA-tagged ubiquitin (MT123) was a generous gift from Dr. Dirk Bohmann (University of Rochester Medical Center).

Experimental design

A total of 48 heterozygous transgenic male rats were divided into four equally sized groups. Beginning at the age of three weeks, rats of each group received resveratrol at the concentration of 50, 100 or 200 μg/ml or normal drinking water as the control. Body weights and water consumption were recorded weekly. At 10 weeks of age, all surviving rats were sacrificed and prostates were removed and weighed. Half of each ventral prostate was immediately frozen in liquid nitrogen for storage until processed. The remainder of each prostate was fixed in formalin and routinely processed for embedding in paraffin and sectioning for H&E staining and histopathological evaluation as well as immunohistochemistry. Testosterone and estradiol levels in serum were analysed by radioimmunoassay in a commercial laboratory (SRL, Tokyo, Japan).

Assessment of prostate neoplastic lesion development

Our TRAP rats showed sequential development of prostatic lesions, i.e. low- and high-grade prostatic intraepithelial neoplasias (PINs) to differentiated adenocarcinomas. Low-grade PIN (LG-PIN) were characterized by having with one or two layers of atypical cells with hyperchromatic nuclei and intact gland profiles and high-grade PIN (HG-PIN) showing increased epithelial stratification with nuclear atypia. Adenocarcinomas were characterized by atypical cells fill almost the lumen of the ducts with cribriform structures or solid growth in acini (Figure 1). The relative numbers of acini with the histological characteristics were quantified by counting for every features, e.g. LG-PIN, HG-PIN and adenocarcinoma, from the total acini in each prostatic lobe and calculated the percentages of each lesions by H&E staining and epithelial contents in acinic areas by performed Azan-Mallory histochemical staining to determine the progression of neoplastic lesions. Red staining areas in the prostates were equivalent to viable epithelial lesions and were quantitatively measured with an Image Processor for Analytical Pathology (IPAP, Sumika Technos Co., Osaka, Japan).

Immunohistochemistry

For Ki-67 immunostaining, deparaffinized sections were incubated with diluted rabbit polyclonal Ki-67 antibody (Novocastra). Apoptotic cells were detected using an In situ Apoptosis Detection Kit (TUNEL method) according to the manufacturer's instructions (Takara Bio Co. Ltd). Labeling indices were counted separately in the ventral, dorsal and lateral prostate and expressed as numbers of Ki-67-positive or TUNEL-positive cells per 100 cells.

Western blot analysis

Cells were lysed in RIPA buffer containing 150 mM NaCl, 1% NP-40, 0.5% sodium deoxycholate, 0.1% SDS, 50 mM Tris-HCl (pH8.0), 0.2 mM sodium orthovanadate and Complete Cocktail (Roche). Cell lysates were electrophoresed through SDS-PAGE gels and blotted onto nitrocellulose membranes. Immunoreactive protein bands were visualized using an ECL plus kit (Amersham Pharmacia Biotech, Freiburg, Germany).

Reverse Transcription-PCR and Real Time-RT PCR

Total RNA was isolated using an RNeasy Mini Kit (Qiagen). Total RNAs were reverse-transcribed with the SuperScript First-Strand Synthesis System (Invitrogen Life Technologies) and amplified by PCR (RT-PCR) using specific primers for AR and GAPDH. Primers used were

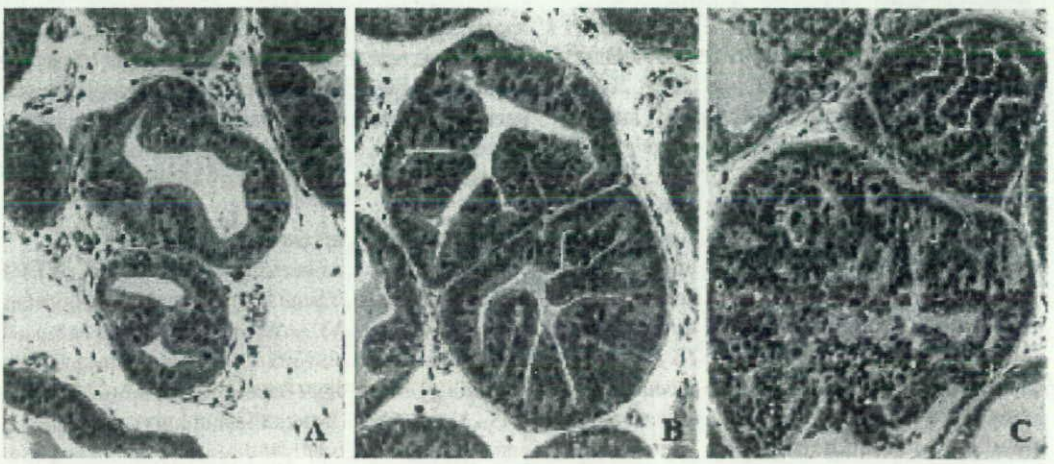

Figure 1. Representative Histopathological Findings for LG-PIN (A), HG-PIN (B) and Adenocarcinoma (C) in Ventral Prostates of TRAP Rats

as follows: (a) AR, forward primer 5-TTGTGAACAGAGTCCCCTAT-3, reverse primer 5-TTCTGGGATGGGTCCTCAGT-3, and (b) GAPDH, forward primer 5-GCGAGATCCCGTCAAGATCA-3, reverse primer 5-CCACAGTCTTCTGAGTGGCAG-3. Real-time quantitative RT-PCR was performed for androgen responsive gene, Gk11 expression using LightCycler (Roche Diagnostics). The primers used to detect GK11 genes are as follows: forward primer 5-GCAGCACCAAACCCCTGGAT-3, reverse primer 5-TGAGATCTGTCACCTTCTCA-3, and primers for rat cyclophilin (used as internal control) are as follows: forward primer 5-TGCTGGACCAAACACAAATG-3, reverse primer 5-GAAGGTGAAAGAAGGCATGA-3.

Reporter gene assay

COS7 cells were transfected with pBKCMV-rAR and pGL3-rPBP-luc using Nucleofector II (Amaxa, Germany). Twenty-four hours after transfection, 10 nM DHT and/or resveratrol was added for another 24 hrs. Cells were lysed with the buffer supplied in the kit 24 hr after transfection. The luciferase assay was conducted using the dual-luciferase reporter assay system (Promega), and the phRL-TK vector (Promega) was used as an internal control. Data shown represent the average and standard deviation of four independent data points.

AR stability assay

COS7 cells were transfected with pBKCMV-rAR, plated into 6-well plate and incubated for 24 hrs. Cells were pretreated with 10 μg/ml cycloheximide for 30 min and then were added 200 μM resveratrol or DMSO. Cells were lysed with RIPA buffer at 0, 1, 2, 4 and 8 hrs after adding resveratrol or DMSO, and cell lysates were subjected to western blot analysis.

Ubiquitylation assay

COS7 cells were transfected with pBKCMV-rAR and MT123 using Nucleofector II, plated into 6-well plates and incubated for 24 hrs. Cells were treated with resveratrol and/or 1 μM MG132 for 24 hrs, and then lysed with IP lysis buffer containing 20 mM Tris-HCl, pH7.5, 150 mM NaCl, 1 mM EDTA, 1 mM EGTA, 1% Triton X-100, 2.5 mM sodium pyrophosphate, 1 mM beta-glycerophosphate, 1 mM sodium orthovanadate, and Complete Cocktail. Immunoprecipitation was performed using rabbit anti-AR antibodies, and subjected to western blot analysis using anti-HA-Tag antibodies.

AR translation assay

COS7 cells were transfected with pBKCMV-rAR using Nucleofector II, seeded into 6-well plate and incubated for 24 hrs. Cells were pretreated with 100, 200 μM resveratrol or DMSO for 13 hrs, and medium was changed to methionine-, cysteine-free RPMI1640/10% FBS with or without resveratrol at 37°C for 1.5 hrs thereafter. Cells were incubated with methionine-, cysteine-free RPMI1640/10% FBS containing 100 μCi/ml Premix [^{35}S]methionine and [^{35}S]cysteine and unlabeled methionine and cysteine (5 μM each) for 1, 2, 4 and 8 hrs. Cold IP lysis buffer was added to each well to lyse cells. One hundred micrograms of cellular protein were immunoprecipitated with rabbit anti-AR antibodies, and samples were subjected to gel electrophoresis, followed by autoradiographic signal quantitation using NIH image software.

Metastasis assay in nude mice

PLS30 cells ($5x10^6$/animal) were injected into the subcutis of 6-week-old male athymic nude mice of the CD-1 strain (Charles River Japan, Inc, Kanagawa). One week after injection, mice were given resveratrol at concentrations of 100 and 200 μg/ml in their drinking water. Six weeks after injection, mice were sacrificed and examined for numbers of metastatic foci in lungs stained with Indian ink (Wexler, 1966).

Statistical analysis.

Data are expressed as means ± SDs. Differences in means between groups were determined by analysis of variance (ANOVA), followed by the Scheffe's post-hoc test with StatView (version 5.0) software (SAS Institute, Inc., Cary, NC). The Spearman's rank correlation coefficient test was used for analysis of dependent data.

Results

Body weight and water consumption

Resveratrol did not cause mortality or non-significant changes in body and relative organ weights (ventral prostate, liver and kidney) compared to the control group. The groups also did not differ in water consumption. Average resveratrol intake was consistent with the doses given, as shown in Table 1.

Testosterone and estradiol levels in serum

Although serum testosterone levels were significantly reduced in the 50 and 100 microgram/ml resveratrol treatment groups compared to control group values, unfortunately we found that the latter were higher than the normal range, which is about 1 - 2 ng/ml (Zeng et al., 2005; Kandori et al., 2005; Cho et al., 2003; Asamoto et al., 2002) (Table 1). Thus, the results were unexplainable regarding effects of resveratrol on serum testosterone. No

Table 1. Serum Testosterone, Estradiol Levels and the Average Resveratrol Intake of TRAP Rats

Treatment	No. of rats	Testosterone (ng/ml)	Estradiol (pg/ml)	Average resveratrol intake (mg/kg/day)
Control	12	4.28±3.15	4.75±1.11	-
Resveratrol 50 ug/ml	12	1.31±0.81*	4.46±1.47	7.59±1.15
Resveratrol 100 ug/ml	12	0.88±0.40*	3.91±0.99	16.11±2.42
Resveratrol 200 ug/ml	12	4.44±2.27	4.79±1.15	30.05±5.90

Data are means ± SD, *, P<0.01 versus control

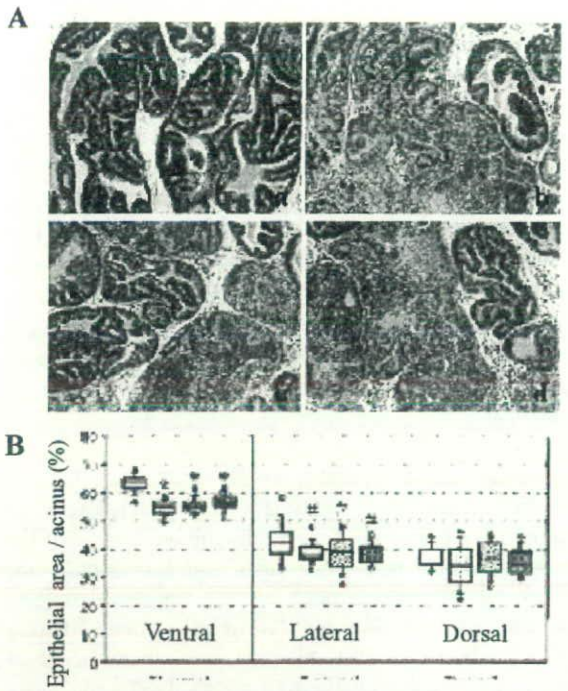

Figure 2. Effects of Resveratrol on Ventral Prostate Adenocarcinomas. (A) Representative histological appearances of (a) control and resveratrol (b) 50 (c) 100 and (d) 200 ug/ml (H &E staining). (B) Quantitative analysis of relative epithelial areas within prostatic acini of TRAP rats. Data are means ± SD for 12 animals. *, P < 0.01 versus control. #, P < 0.05 versus control (Spearman 's rank correlation coefficient test). Boxes left to right: Control; resveratrol 50;100; 200 ug/ml

significant changes were noted in serum estradiol levels compared to controls (Table 1).

Effects of resveratrol treatment on development of neoplastic lesions in the prostate

There were partial pathologic responses to resveratrol treatment as demonstrated by reduction in the content of prostatic neoplastic lesions in TRAP rats (Figure 2A). However, small foci of carcinoma remained, so that there were no significant differences in the incidences of PIN or adenocarcinoma in the prostates of TRAP rats (Table 2). There were no adenocarcinomas in the dorsal and anterior lobes in all groups of rat. As the entire ventral and lateral prostate lobes were occupied with tumor lesions and clear differences in prostate adenocarcinoma incidence were not observed among the groups, we evaluated the areas of epithelium including tumors morphometrically. The results, as summarized in Figure 2B, showed that resveratrol treatment significantly suppressed neoplastic lesion development about 14%, even at low dose (50 μg/ml) in the ventral lobes and also in the lateral lobes with a dose-dependent manner. Furthermore, evaluation of the proportion of preneoplastic and neoplastic lesions showed that resveratrol tended to shift the progression of neoplastic growth by suppressed the number of adenocarcinoma and HG-PIN and consequently, increased LG-PIN in all lobes (Table 3). The numbers of apoptotic cells in the ventral prostate of rats treated with resveratrol were also significantly increased as compared with the controls, while there were no obvious differences in Ki-67 labeling indices (Table 4).

Resveratrol downregulates AR and Gk11 in the ventral prostate

Figure 3A shows that resveratrol clearly suppressed AR protein expression even at low dose of 50 μg/ml and also slightly suppressed SV40 Tag expression at the high dose. RT-PCR analysis of the AR gene showed no obvious differences at the AR mRNA level (Figure 3B), suggesting post-transcriptional downregulation. However, mRNA expression of the androgen responsive gene, Gk11, was significantly suppressed in the ventral prostate (Fig 3C).

Resveratrol affects AR function and its stability in vitro

In COS7 cells transfected with pBKCMV/rAR, resveratrol repressed exogenous AR expression, as well as endogenously in the LNCaP cells (Figure 4A). Subsequent reporter assays clearly demonstrated inhibition of functional AR activity in a dose-dependent manner, this being considered to simply reflect downregulation of AR protein expression by resveratrol. In resveratrol-treated cells, the half-life of AR protein was also slightly reduced, with a one hour difference compared to control cells (Figure 4B), suggesting an influence on AR protein degradation. The suppressive effect of resveratrol was not

Table 2. Incidences of Prostate Adenocarcinomas in TRAP Rats Treated with Resveratrol

Treatment	No. of rats	Incidence of adenocarcinoma (%)			
		Ventral	Lateral	Dorsal	Anterior
Control	12	11 (92)	4 (33)	0	0
Resveratrol 50 ug/ml	12	10 (83)	2 (17)	0	0
Resveratrol 100 ug/ml	12	10 (83)	5 (42)	0	0
Resveratrol 200 ug/ml	12	9 (75)	2 (17)	0	0

Table 3. Quantitative Evaluation of Neoplastic Lesions in Prostate of TRAP Rats Treated with Resveratrol

Treatment	No. of rats	Relative number of acini with histological characteristics(%)								
		Ventral			Lateral			Dorsal		
		LG-PIN	HG-PIN	Carcinoma	LG-PIN	HG-PIN	Carcinoma	LG-PIN	HG-PIN	Carcinoma
Control	12	3.1±1.0	95.3±1.0	1.6±0.5	20.7±12.0	77.6±11.4	1.7±1.6	24.4±10.8	75.6±10.8	-
Resveratrol 50 ug/ml	12	4.8±2.2*	93.9±1.9*	1.3±0.5#	23.5±11.3	75.8±11.0	0.6±0.6*	31.7±20.1	68.3±20.1	-
Resveratrol 100 ug/ml	12	3.7±1.4	95.1±1.5	1.2±0.4*#	18.7± 8.0	80.6± 7.7	0.6± 0.7	28.6±12.0	71.4±12.0	-
Resveratrol 200 ug/ml	12	4.0±1.5	94.9±1.4	1.1±0.4*#	22.9± 9.2	76.5± 9.3	0.6±0.9	30.7±16.7	69.3±16.7	-

Data are mean ± SD *, P<0.05 versus control #, P<0.05 versus control (Spearman's rank correlation coefficient test)

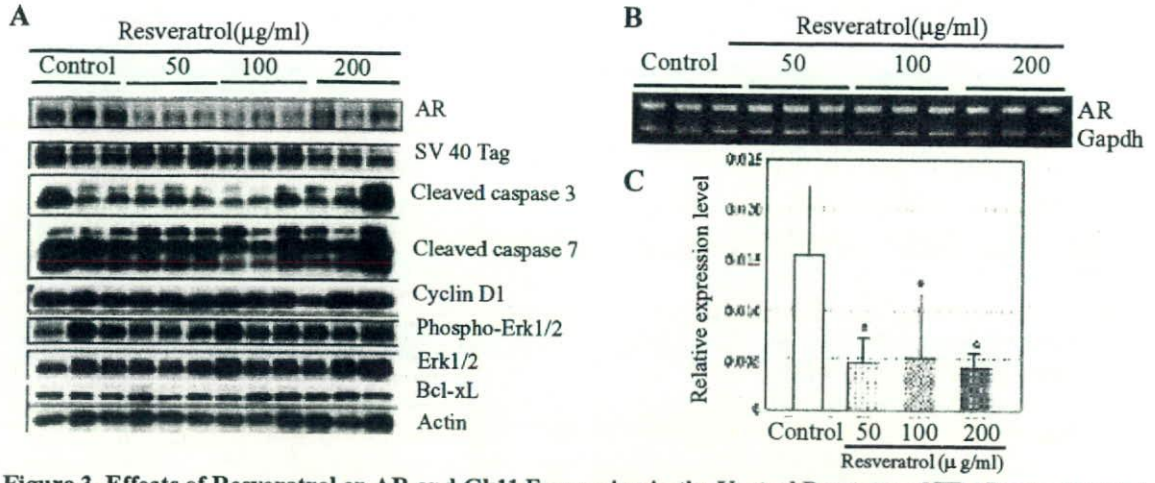

Figure 3. Effects of Resveratrol on AR and Gk11 Expression in the Ventral Prostates of TRAP rats. (A) Western blot analysis for AR, MAPK and apoptosis-related proteins; (B) RT-PCR analysis for AR; (C) Real Time-RT PCR analysis for Gk11 expression normalized to cyclophilin used as an internal control. Data are means ± SD of five animals. *, $P < 0.05$ versus control

completely blocked by the proteasome inhibitor, MG132 (Figure 4C), suggesting that resveratrol-induced AR protein down-regulation is not mainly via the proteasome-dependent pathway.

Resveratrol suppresses AR translation in vitro

To further determine the possible mechanism involved in the regulation of AR expression at the posttranscriptional level, AR-translation *in vitro* assay was performed to characterize whether resveratrol affects AR protein translation efficiency. Figure 4D shows that treatment with resveratrol reduced AR protein synthesis by about 40% as compared with untreated cells. This inhibitory phenomena might be specific on AR protein translation because resveratrol did not affected the translation of ERK1 and Cyclin D1, which been chosen as control protein, using LNCaP cells (data not shown).

Effects of resveratrol on lung metastasis in nude mice

There were no significant differences in growth of

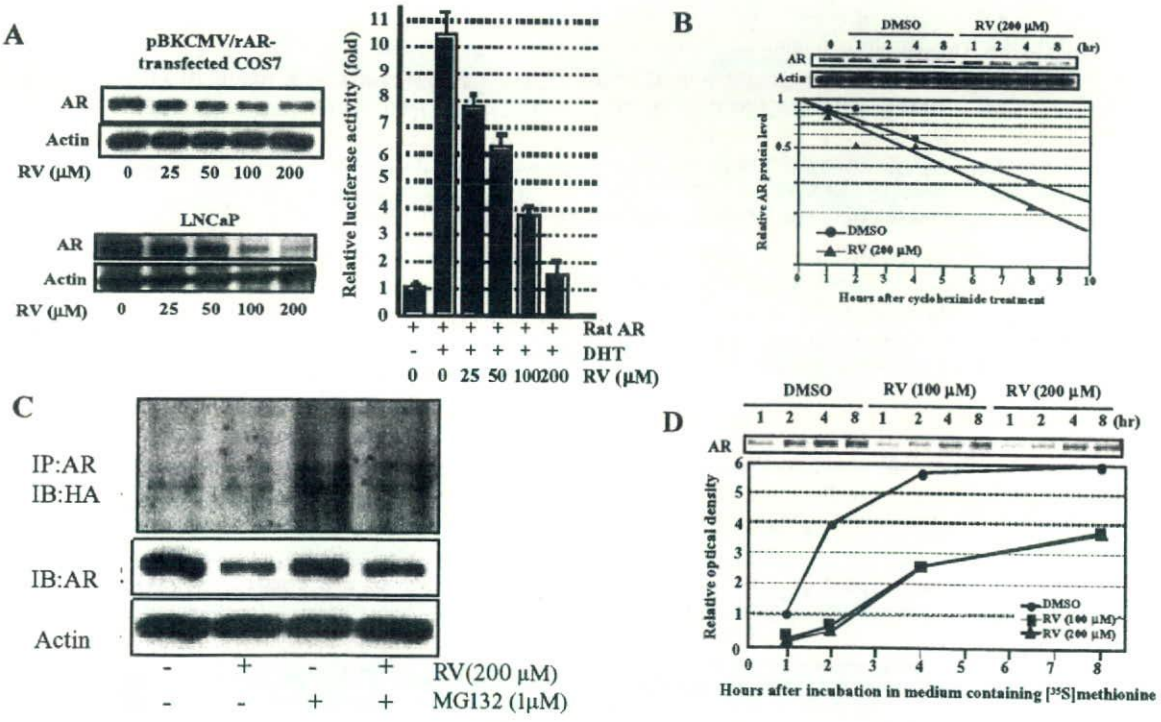

Figure 4. Mechanisms of Down-regulation of AR Protein by Resveratrol. (A) *Left panel*, western blot analysis of AR in transiently pBKCMV/rAR-transfected COS7 cells (top) and in LNCaP cells (*below*). *Right panel*, Reporter gene assay for AR. Means ± SD. (B) AR protein stability assay of COS7 cells transfected with pBKCMV/rAR, pretreated with cycloheximide and then treated with 200 uM resveratrol or DMSO. AR protein levels were determined by western blot analysis and normalized to actin (*top*). The AR expression was quantified and plotted relative to time 0. (C) Ubiquitylation assay for AR in COS7 cells transfected with both pBKCMV/rAR and pMT123 (HA-Ub), treated with resveratrol and/ or MG132. (D) AR translation assay of COS7 cells transfected with pBKCMV/rAR and incubated for 24 hrs. Details are described in the *Materials and Methods*

Table 4. Ki-67 Labeling index (%) and Apoptotic Indices in Prostate of TRAP Rats Treated with Resveratrol

Treatment	No.	Ki-67 labeling			Apoptotic index (%)		
	of rats	Ventral	Lateral	Dorsal	Ventral	Lateral	Dorsal
Control	12	22.6±3.3	23.0±4.8	14.1±3.2	3.6±1.2	2.7±1.1	0.9±0.3
Resveratrol 50 ug/ml	12	23.7±6.0	23.3±6.0	14.8±3.7	5.5±1.9*	2.9±1.0	0.8±0.3
Resveratrol 100 ug/ml	12	22.0±4.4	22.1±3.9	15.1±3.9	5.4±1.9*	3.6± 1.8	0.9±0.3
Resveratrol 200 ug/ml	12	20.6±4.0	26.0±6.7	17.4±3.8	5.4±1.6*	2.4±1.2	0.8±0.2

Data are mean ± SD *, P<0.01 versus control

xenografts or lung metastases after subcutaneous injection of the PLS30 cell line into the flanks of athymic nude mice and treatment with resveratrol (Table 5).

Discussion

There was no report regarding the effectiveness of resveratrol in preclinical animal model of prostate cancer so far (Syed et al., 2007). The present study demonstrated, for the first time to our knowledge, suppressive effects of resveratrol on prostate cancer growth and induction of apoptosis through AR down-regulation in an *in vivo* rat model. This *in vivo* finding is an important step in verifying potential chemoprevention by resveratrol before recommending use in humans. Well-designed *in vivo* animal study plays a critical role between the *in vitro* experiment and clinical trials especially for the optimal dosing and toxicity of the agent. Importantly, the inhibition effect was achieved without any significant change in final body weights, relative liver and kidney weights and water consumption. Lack of signs of toxicity in the present experiment is in line with the earlier finding that oral intake of high dose (20 mg/kg/day) of resveratrol is not harmful to rats (Juan et al., 2002), although the dosage of resveratrol employed in this study was equivalent to 400 - 1,600 times the amount consumed by a person with ordinary wine intake (Gescher and Steward, 2003). The previous report showed that serum concentration of free, 3- and 4'-glucuronide of resveratrol in healthy human with moderate consumption of red wine were up to 26 nM, 190 nM and 2.2 uM, respectively (Vitaglione et al., 2005), and we used the dose of resveratrol that was equivalent to about 100 times concentration compared to these human data in *in vitro* study.

Resveratrol is well known for its phytoestrogenic and antioxidant properties (Baur and Sinclair, 2006) and exerts a variety of beneficial effects in humans, such as protection against the metabolic syndrome (Lagouge et al., 2006), inflammation and viral infection (Friel and Lederman, 2006). Recently it was also shown to have a possible positive influence on life-expectancy, since food supplementation with resveratrol prolonged lifespan and retarded the expression of age-dependent traits in a short-lived vertebrate (Valenzano et al., 2006; Baur et al., 2006). A population-based case-control study further suggested that consumption of red wine may be associated with a reduction of the relative risk of prostate cancer (Schoonen et al., 2005) and resveratrol is probably one of the main microcomponents of wine responsible. The suppressive effect on AR expression by resveratrol in our study is agreement with earlier *in vitro* findings (Jones et al., 2005; Hsieh and Wu, 2000; Mitchell et al., 1999), as well as the hypothesis that resveratrol results in scavenging of incipient populations of androgen-dependent prostate cancer cells through its influence on the AR (Kyprianou and isaacs, 1988). *In vitro* studies have also indicated that resveratrol has marked antiandrogenic effects, in the androgen-dependent human prostate cell line LNCaP, that involve suppression of AR, the AR-specific co-activator ARA70 and various AR-regulated genes and that these effects are associated with reduced cell-growth and induction of apoptosis (Mitchell et al., 1999).

It is of clear interest that resveratrol not only downregulated the AR in our TRAP model but also suppressed the androgen responsive gene, Gk11, known as the ortholog of human PSA, at the mRNA level. This *in vivo* finding reflect that resveratrol suppressed AR pathway functionally in prostatic lesions of TRAP rats that might similar to affect PSA in human condition, such as the effect of anti-androgen drugs suppressed PSA level that paralleled with cancer growth inhibition by interrupting AR signal pathways in prostate cancer patients.

Resveratrol is also known to suppress late stage processes of carcinogenesis such as angiogenesis and metastasis. For example, resveratrol was able to directly inhibit the gelatinolytic activities of MMP2 and MMP9 which are associated with tumor metastasis (Banerjee et al., 2002). However, effects in cell culture may not directly reflect whole body systems in animal systems and administration of 1-5 mg per kg (body weight) daily of resveratrol in one study failed to affect the growth or metastasis of breast cancer in mice, despite promising *in vitro* results (Bove et al., 2002). In the present investigation, resveratrol similarly did not reduce lung metastasis in mice bearing prostate carcinoma tumors, possibly because the PLS30 cells used are negative for AR protein and show and androgen-independent

Table 5. In Vivo Growth and Lung Metastasis of PLS30 rat Prostate Cancer Cells in Nude Mice Treated with Resveratrol

Treatment	No. of mice	Tumor volume of xenograft(cm^3)	No. of metastatic foci in lungs
Control	11	0.96 ± 0.49	50.6 ± 38.9
Resveratrol 100 ug/ml	10	1.10 ± 0.47	35.0 ± 24.5
Resveratrol 200 ug/ml	10	0.85 ± 0.40	38.2 ± 28.5

Data are means ± SD

phenotype (Nakanishi et al., 1996). Thus, effects of resveratrol are more likely to be AR-dependent. Understanding the molecular mechanisms of resveratrol mediated downregulation of AR signaling may aid in the development of effective chemoprevention since the receptor plays a major role in the initiation and progression of prostate cancer (Sadi et al., 1991). The observed unique effects of resveratrol on AR protein point to possible optimization of chemopreventive effect in future by use in combination with other agents such as vitamin E (Zhang et al., 2002) and selenium (Chun et al., 2006).

In conclusion, our *in vivo* results clearly demonstrated that resveratrol can inhibit prostate carcinogenesis with induction of apoptosis through AR down-regulation, without any signs of tissue-toxicity. Our findings provide support for previous in vitro data as well as population-based case-control study suggesting that resveratrol intake through wine associated with the reduction of the relative risk of prostate cancer. Our findings and the fact that most prostate cancers are initially androgen-dependent suggest that resveratrol warrants further examination with the eventual aim of clinical testing.

Acknowledgments

This work was supported by a Grant-in-Aid for Cancer Research from the Ministry of Health, Labour and Welfare of Japan, a Grant-in-Aid for the 2nd Term Comprehensive 10-Year Strategy for Cancer Control from the Ministry of Health, Labour and Welfare of Japan, a grant from the Japan Food Chemical Research Foundation, and a grant from the Society for Promotion of Pathology of Nagoya, Japan.

References

Asamoto M, Hokaiwado N, Cho YM, et al (2001a). Prostate carcinomas developing in transgenic rats with SV40 T antigen expression under probasin promoter control are strictly androgen dependent. *Cancer Res*, **61**, 4693-700.

Asamoto M, Hokaiwado N, Cho YM, et al (2001b). Metastasizing neuroblastomas from taste buds in rats transgenic for the Simian virus 40 large T antigen under control of the probasin gene promoter. *Toxicol Pathol*, **29**, 363-8.

Asamoto M, Hokaiwado N, Cho YM, et al (2002). Effects of genetic background on prostate and taste bud carcinogenesis due to SV40 T antigen expression under probasin gene promoter control. *Carcinogenesis*, **23**, 463-7.

Aggarwal BB, Bhardwaj A, Aggarwal RS, et al (2004). Role of resveratrol in prevention and therapy of cancer: preclinical and clinical studies. *Anticancer Res*, **24**, 2783-840.

Aziz MH, Kumar R, Ahmad N (2003). Cancer chemoprevention by resveratrol: in vitro and in vivo studies and the underlying mechanisms (review). *Int J Oncol*, **23**, 17-28.

Baur JA, Sinclair DA (2006). Therapeutic potential of resveratrol: the in vivo evidence. *Nat Rev Drug Discov*, **5**, 493-506.

Baur JA, Pearson KJ, Price NL, et al (2006). Resveratrol improves health and survival of mice on a high-calorie diet. *Nature*, **444**, 337-42.

Banerjee S, Bueso-Ramos C, Aggarwal BB (2002). Suppression of 7,12-dimethylbenz(a)anthracene-induced mammary carcinogenesis in rats by resveratrol: role of nuclear factor-kappaB, cyclooxygenase 2, and matrix metalloprotease 9. *Cancer Res*, **62**, 4945-54.

Bhat KP, Pezzuto JM (2002). Cancer chemopreventive activity of resveratrol. *Ann N Y Acad Sci*, **957**, 210-29.

Bove K, Lincoln DW, Tsan MF (2002). Effect of resveratrol on growth of 4T1 breast cancer cells in vitro and in vivo. *Biochem Biophys Res Commun*, **291**, 1001-5.

Cho YM, Takahashi S, Asamoto M, et al (2003). Age-dependent histopathological findings in the prostate of probasin/SV40 T antigen transgenic rats: lack of influence of carcinogen or testosterone treatment. *Cancer Sci*, **94**, 153-7.

Chun JY, Nadiminty N, Lee SO, et al (2006). Mechanisms of selenium down-regulation of androgen receptor signaling in prostate cancer. *Mol Cancer Ther*, **5**, 913-8.

Delmas D, Lancon A, Colin D, et al (2006). Resveratrol as a chemopreventive agent: a promising molecule for fighting cancer. *Curr Drug Targets*, **7**, 423-42.

Friel H, Lederman H (2006). A nutritional supplement formula for influenza A (H5NCancer Epidemiol Biomarkers Prev, 16, 2193-2203.Cancer Epidemiol Biomarkers Prev, 16, 2193-2203) infection in humans. *Med Hypotheses*, **67**, 578-87.

Gescher AJ, Steward WP (2003). Relationship between mechanisms,bioavailibility, and preclinical chemopreventive efficacy of resveratrol: a conundrum. *Cancer Epidemiol Biomarkers Prev*, **12**, 953-7.

Hsieh TC, Wu JM (2000). Grape-derived chemopreventive agent resveratrol decreases prostate-specific antigen (PSA) expression in LNCaP cells by an androgen receptor (AR)-independent mechanism. *Anticancer Res*, **20**, 225-8.

Jang M, Cai L, Udeani GO, et al (1997). Cancer chemopreventive activity of resveratrol, a natural product derived from grapes. *Science*, **275**, 218-20.

Jemal A, Siegel R, Ward E, et al (2007). Cancer statistics. *CA Cancer J Clin*, **57**, 43-66.

Jones SB, DePrimo SE, Whitfield ML, et al (2005). Resveratrol-induced gene expression profiles in human prostate cancer cells. *Cancer Epidemiol Biomarkers Prev*, **14**, 596-604.

Juan ME, Vinardell MP, Planas JM (2002). The daily oral administration of high doses of trans-resveratrol to rats for 28 days is not harmful. *J Nutr*, **132**, 257-60.

Kandori H, Suzuki S, Asamoto M, et al (2005). Influence of atrazine administration and reduction of calorie intake on prostate carcinogenesis in probasin/SV40 T antigen transgenic rats. *Cancer Sci*, **96**, 221-6.

Kato K, Takahashi S, Mori T et al (1998). Establishment of transplantable rat prostate carcinomas from primary lesions induced by 3,2'-dimethyl-4-aminobiphenyl and testosterone. *J Toxicol Pathol*, **11**, 27-32.

Kyprianou N, Isaacs JT (1988). Activation of programmed cell death in the rat ventral prostate after castration. *Endocrinology*, **122**, 552-62.

Lagouge M, Argmann C, Gerhart-Hines Z, et al (2006). Resveratrol improves mitochondrial function and protects against metabolic disease by activating SIRT1 and PGC-1alpha. *Cell*, **127**, 1109-22.

Mitchell SH, Zhu W, Young CY (1999). Resveratrol inhibits the expression and function of the androgen receptor in LNCaP prostate cancer cells. *Cancer Res*, **59**, 5892-5.

Nakanishi H, Takeuchi S, Kato K, et al (1996). Establishment and characterization of three androgen-independent, metastatic carcinoma cell lines from 3,2'-dimethyl-4-aminobiphenyl-induced prostatic tumors in F344 rats. *Jpn J Cancer Res*, **87**, 1218-26.

Palamara AT, Nencioni L, Aquilano K, et al (2005). Inhibition of influenza A virus replication by resveratrol. *J Infect Dis*, **191**, 1719-29.